

W-AM-Sym-1 PROTEIN FOLDING INSIDE MEMBRANE BILAYERS. D.M. Engelman, B.D. Adair, J.F. Hunt, T.W. Kahn and J.-L. Popot*, Dept. of Molecular Biophysics and Biochemistry, Yale University; *College de France and Institut de Biologie Physico-Chimique, France.

We hypothesize that the folding of many transmembrane proteins can be conceptually divided into two energetically distinct processes. In the first stage, independently stable transmembrane helices form, mainly in response to the hydrophobic effect and polypeptide chain hydrogen bonding. In the second stage, the helices interact with each other as part of the structure of a functional transmembrane protein. Interactions potentiating the second stage include electrostatic effects and packing considerations as the major determinants. We have developed a number of experimental approaches to study the formation and interaction of transmembrane helices in the folding of bacteriorhodopsin and in other systems. These experiments support the basic notions embodied in the two stage model.

Experimental results will be presented concerning the structures formed by subfragments of the bacteriorhodopsin molecule when the fragments are independently inserted in lipid bilayers. As predicted by the two stage model, these fragments form transmembrane helices even in the absence of other portions of the bacteriorhodopsin molecule. To study the second stage, we use an experiment developed by Popot (1): the bacteriorhodopsin molecule is divided into two fragments, the fragments are independently inserted in two populations of lipid vesicles, and the fragments then are allowed to interact by fusing a mixture of the vesicles in solution. This process results in the interaction of the two fragments and the rebinding of retinal to obtain a native absorption spectrum. The resulting molecule is functional. By varying the environment and the sequence of the molecule, factors in the reassociation can be studied.

Helix-helix interactions within bilayers are of key importance in the folding of many membrane proteins and, we believe, in the process of oligomerization of membrane proteins as well. This point will also be discussed.

1. *J. Mol. Biol.* (1987) 198, 655.

W-AM-Sym-2

MINIMALLY DESIGNED PEPTIDE ION CHANNELS

James D. Lear, Z. R. Wasserman, and W. F. DeGrado

Ion channel proteins appear to be composed of transmembrane α -helices, some of which contain sequences which define a "face" of polar residues. These amphiphilic helices, in association with others, can provide a conduction pathway across a lipid bilayer. To explore this idea with a minimal complexity system, model peptides containing only leucine and serine residues were synthesized and characterized. Two different heptad repeat units, LSLLSL and LSSLSS, assembled into 21 residue peptides, produced well-defined single ion channel activity in planar bilayers. The conductance and lifetime properties of these channels will be discussed in relation to the structural principles underlying their design.

W-AM-Sym-3 CONFORMATION, ORIENTATION, AND ACCUMULATION OF REGULATORY PEPTIDES ON LIPID MEMBRANES: KEY TO RECEPTOR SELECTIVITY by Robert Schwyzer (Intr. by Stephen H. White), Swiss Federal Institute of Technology (ETH), CH-8093 Zürich, Switzerland.

Regulatory peptides are of vital importance as neurotransmitters, neuromodulators, hormones, immunomodulators, and cell-growth factors. Their biologic effects are mediated through selective reactions with specific membrane-bound receptors and receptor subtypes. Such reactions often occur *via* a membrane-associated state of the peptide. From infrared studies on thin lipid films and studies with vesicle-mediated photolabelling, my coworkers and I have shown that several ligands of the opioid κ receptor, the melanotropin steroidogenic receptor, and the neurokinin NK-1 receptor insert their "message" segments as an α -helix, more or less perpendicularly, into the membrane (similar behavior has been confirmed for other peptides with NMR techniques by Miyazawa). The binding parameters for these membrane-associated states were determined from the capacitance minimization potential of lipid bilayers. I have developed a theory to account for the observed binding constants and the preferred conformation and orientation of these peptides. In contrast to the receptor subtypes mentioned above, ligands of the opioid μ and δ , the melanotropic melanophore receptors, and the neurokinin NK-2 and NK-3 receptors are predicted not to form the inserted α -helical structure. A selection between the μ and δ (or NK-2 and NK-3) receptors appears to be made on the basis of an electrostatic gradient near the membrane surface. Quantitative correlations of estimated parameters of peptide-membrane interaction with biologic data suggest that the molecular mechanism of receptor selection may be based to a large extent on the membrane-induced compartmentalization of the ligands for the different receptors.

W-AM-Sym-4 INTERFACIAL HYDROPHOBICITY AND THE INSERTION OF TRANSBILAYER HELICES INTO LIPID BILAYERS. Stephen H. White and Russell E. Jacobs, Department of Physiology and Biophysics, University of California, Irvine, CA 92717

Our laboratories are engaged in studies of the physical chemistry of peptide/bilayer interactions in order to understand the mechanism of insertion of transbilayer helices. Our basic approach is to relate thermodynamic measurements to structural parameters obtained by NMR and neutron diffraction methods. We describe the results of this approach for tripeptides of the form A-X-A-O-tert-butyl where X=G, A, L, F, and W. We show that (1) the transfer of the tripeptides from water to DMPC vesicles ($T > T_M$) is purely entropy-driven ($\Delta H=0$, $\Delta S > 0$) as expected for hydrophobic interactions, (2) the Trp peptide is located exclusively at the DOPC bilayer interface, (3) about 60% of the available hydrophobic free energy is consumed upon binding, and (4) the binding leads to the incorporation of a small but significant amount of water within the hydrocarbon core of the bilayer. The first three observations suggest that interfaces provide a very favorable environment for peptides. A thermodynamic analysis of insertion using the interface as a reference phase indicates that the interface is likely to be important in helix formation and insertion, emphasizes the importance of intrahelical hydrogen bonds in insertion, and leads to a "floating" hydrophobicity scale which allows one to consider explicitly the status of side chain hydrogen bonds in transbilayer helix searches. Supported by the NSF and Am. Heart Assoc. REJ is an Established Investigator of the Am. Heart. Assoc.

W-AM-Min-1 HYDRATION AND THE STRUCTURE OF PROTEINS FROM COMPUTER SIMULATIONS. William L. Jorgensen and Julian Tirado-Rives, Department of Chemistry, Purdue University, West Lafayette, Indiana 47907.

A 100 ps molecular dynamics simulation has been carried out for the proteinase inhibitor from the third domain of silver pheasant ovomucoid (OMSVP3) in a periodic cell with ca. 1700 water molecules. The calculations have permitted evaluation of the quality of the AMBER/OPLS force field for proteins, the differences between the computed solution structure for OMSVP3 and Huber's crystal structure, and many details on the hydration of protein constituents. Roughly 30 ps was required for the protein to equilibrate after which the rms deviation between the solution and crystal structures for the backbone atoms converged to 1.4 - 1.5 Å, a result comparable to the 1.2 Å deviation found for two crystal structures of BPTI. The last residue of the α -helix in the crystal, Ser-44, does not form the required hydrogen bond with Ala-40 to be a part of the helix in solution, as in the crystal for Japanese quail ovomucoid. Among numerous other observations, in solution the β -sheet for OMSVP3 is not found to contain a third strand. Highlights from complete hydrogen bonding inventories will also be discussed.

W-AM-Min-2 HYDRATION PATTERNS IN CRAMBIN AT ATOMIC RESOLUTION.

Martha M. Teeter, Department of Chemistry, Boston College, Chestnut Hill, MA 02167.

The hydrophobic protein crambin (MW 4700) forms crystals which diffract to atomic resolution (0.83 Å) and which at 140 K have all of the solvent ordered. This crystal structure provides an opportunity to study in atomic detail both the water environment surrounding each amino acid at the protein surface and the organization of water layers adjacent to the protein surface. Water is important in stabilizing a protein in its folded conformation and also is necessary for an enzyme to be active.

Two general types of water networks are found in crambin crystals: chains connecting polar atoms and pentagonal water rings at a hydrophobic protein surface. Such linked waters have been seen in a number of protein crystal structures, where the first layer of water is well-ordered. The protein crambin is the first where a cluster of pentagonal rings of water molecules were found. Some chains of water in continuous alternate networks also contain five- and six-membered rings.

There is a question as to whether the arrangement of water at the protein surface is determined by the amino acid geometry or by the water itself. Pure liquid water has been modeled as primarily five- and six-membered rings that form and break continuously. Ice forms six-membered, chair structures. The pentagonal rings of water in crambin, although hydrogen bonded to the protein, have more contacts to other waters than to the protein. Hence, in terms of their neighbors (and ring structure), they resemble water more than the protein surface. In contrast, the chain-like water arrays are strongly influenced by the protein surface. Patterns in the binding of waters to hydrophilic residues suggest that their positions could be predicted for any protein structure from the side chain geometry.

W-AM-Min-3 SOLVENT STRUCTURE THEMES IN CRYSTALS OF TRYPSIN. J. Finer-Moore, J. Hurley, and R. Stroud. Dept. of Biochemistry, University of California, San Francisco, CA 94143.

We describe a method for refining the solvent structure including the disordered solvent region in the X-ray crystal structure of DIP-inhibited trypsin. The water structure so determined is compared to the solvent structure independently derived by neutron diffraction. The ordered solvent in the X-ray crystal structures of several other crystal forms of trypsin and trypsinogen, including a rat trypsin mutant, are compared. Our results show that many water positions are conserved between homologous structures, and that many waters involved in intramolecular contacts in at least one structure are conserved in different crystal forms. General characteristics of water structure and the possible significance of the conserved waters are discussed.

W-AM-Min-4 ROLES OF SOLVENT IN MUTANT T4 LYSOZYME STRUCTURES. Brian W. Matthews, Institute of Molecular Biology, University of Oregon, Eugene, Oregon 97403.

The lysozyme of phage T4 is being used as a model system to investigate the structural basis of the thermodynamic stability of proteins. A collection of randomly-generated temperature-sensitive mutants has been isolated and characterized to locate residues that contribute to stability. Other mutant lysozymes, generated by site-directed methods, permit the importance of the hydrophobic effect, hydrogen-bonds, and other interactions to be quantitated in a systematic manner. Crystal structure analyses of many mutant lysozymes has shown that the ability of proteins to undergo conformational changes makes them surprisingly tolerant of amino acid substitutions.

In mutant T4 lysozyme structures there are often changes in solvent structure associated with the amino acid substitution. These changes serve to illustrate the different roles of bound solvent. In some cases a water molecule is observed to occupy a cavity created by the replacement of a larger amino acid with a smaller one. In other cases a bound water molecule can mimic the role of a polar amino acid side-chain. Solvent molecules are also seen to be intimately involved with intermolecular contacts that are essential for crystallization of the protein. Bound solvent and/or bound counterions are also seen to contribute to the stabilization of alpha-helix dipoles.

W-AM-Min-5

WATER, INHIBITOR BINDING AND THE TRANSITION STATE AFFINITY OF ENZYMES R.

Wolfenden, W. M. Kati, and L. Frick, Dept. of Biochemistry, University of North Carolina, Chapel Hill, N. C. 27514

The catalytic function of an enzyme depends on its ability to discriminate between the substrate in the ground state and the altered substrate in the transition state, binding the latter species more tightly and diminishing the difference in free energy that limits the rate of reaction. These two forms of the substrate share many structural elements, so that discrimination is presumably based on a few structural differences in the immediate neighborhood of bonds that are formed and broken during the reaction. Recent nmr and uv experiments imply that a single hydroxyl group can, by its presence, enhance the binding affinity of a transition state analog for adenosine deaminase by a factor of 10^8 , and similar evidence has now been gathered for cytidine deaminase. The free energy of binding of inhibitors, after correction for the free energy needed to extract the hydroxyl group from solvent water, appears commensurate with values for the formation of a single hydrogen bond between a hydroxyl group and a charged carboxylate group in the vapor phase. The orientation of the critical hydroxyl group will be discussed, along with some possible consequences of "trapping" water molecules, and of enzyme distortion, when inhibitors are bound.

W-AM-A1 CONDUCTIVITY DISCONTINUITY AT FERROELECTRIC PHASE TRANSITIONS AS POSSIBLE SOURCE OF CHANNEL UNITARY CONDUCTANCE CHANGES. H. Richard Leuchtag, Department of Biology, Texas Southern University, Houston, TX 77004.

The ferroelectric electrodiffusion hypothesis provides a physical explanation of I-V hysteresis, cold and heat block, currents activated by temperature changes and mechanical stimuli, voltage-dependent birefringence, gating currents and the origin of an action potential by a depolarizing stimulus [Ferroel., Oct. 1988; *J. Theor. Biol.* 127:321-340, 341-359 (1987)]. The abrupt changes in channel conductance observed in single-channel experiments are also consistent with this hypothesis. As shown by V. M. Gurevich [*Electric Conductivity of Ferroelectrics* (Jerusalem 1971)], ferroelectrics such as triglycine sulfate exhibit discontinuous changes in conductivity at the transition temperature (Curie point). Since a depolarization lowers the transition temperature, this effect, applied to a ferroelectric channel unit, implies a conductance change at threshold, when the transition temperature has been lowered to the actual temperature of the channel. Thus the ferroelectric electrodiffusion hypothesis provides a physical explanation of the unitary conductance changes observed in Na and other excitable channels.

W-AM-A2 ION CONDUCTION CHARACTERISTICS OF BATRACHOTOXIN-MODIFIED SODIUM CHANNELS FROM FROG MUSCLE. David Naranjo, Osvaldo Alvarez, and Ramon Latorre. Departamento de Biología, Facultad de Ciencias, Universidad de Chile, Santiago, Chile and Centro de Estudios Científicos de Santiago, Santiago, Chile.

Most of the studies on sodium currents in skeletal muscle have been done in amphibian muscles. However, very little is known about the characteristics of the individual sodium channels in this preparation. With the purpose to obtain a better understanding of this type of sodium channels, a muscle membrane preparation, enriched in transverse tubule, was made from skeletal muscle of the Chilean frog *Caudivertera caudivertera*. Single sodium channels from frog muscle were incorporated into planar bilayers in the presence of 200 nM batrachotoxin (BTX). The BTX-modified channel is blocked by nanomolar concentrations of tetrodotoxin and saxitoxin. In symmetrical 200 mM NaCl, at 22°C, channel conductance is 10 pS, but another more conductive (15 pS) substate also appears although infrequently. This larger conductance open substate appears more frequently as the sodium concentration is reduced and becomes predominant in the sodium concentration range of 0.4 to 1 mM Na⁺. At 0.4 mM Na⁺ the conductance of the open substates is 4 and 6 pS. Neither the large nor the smaller substate conductance vs [Na⁺] curves can be fitted by a simple Langmuir isotherm. However, the data is well explained by a three-barriers two-well model which incorporates a fixed charge at the channel entrances. A good fit to the data was obtained by making the wells -8 kT for both substates, the peaks 5.2 kT for the smaller conductance substate and 5.0 kT for the larger conductance substate, and a fixed charge density at the channel entrances of one electronic charge per 2700 Å².

Supported by NIH grant GM-35981, Fondo Nacional de Investigación Grant 1988-0451, and Universidad de Chile DTI Grants B-2805/8812 and B-2809/8813.

W-AM-A3 PROPERTIES OF SINGLE, VOLTAGE-ACTIVATED PURIFIED AND RECONSTITUTED EEL Na CHANNELS. A. M. Correa, W. S. Agnew, and F. Bezanilla. Cellular and Molecular Physiology, Yale Univ. Sch. of Med., New Haven, CT 06510; Dept. of Physiol., UCLA, Los Angeles, CA 90024, and MBL, Woods Hole, MA.

We report the characteristics of single Na channels purified from *Electrophorus electricus* and reconstituted into liposomes (PE:PS:PC, 5:4:1). Channels were purified by ion exchange and lectin affinity chromatography (James and Agnew, *Bioophys. J.* 53:15a, 1988), and reconstituted by removing the detergent from lipid supplemented samples. The liposomes containing the purified channels were prepared for single channel recording from excised patches as described by Correa and Agnew (*Bioophys. J.* 54:569, 1988). The external side of the channels studied faced the inside of the pipette. The convention for voltage and sidedness of the solutions in the excised patch follows the orientation of the channel. Recordings were performed at room temperature (18-20°C) in 250 mM NaCl inside and with 250 mM variable cationic composition outside.

The conductance, determined from the slope of I-V curves, ranges between 15 and 30 pS depending on the cations present in the external solution. The channel is selective for Na⁺ over K⁺, Rb⁺ and Cs⁺. Typically, hyperpolarizing holding potentials of < -100 mV were required to elicit channel activity. The activation curve appears displaced towards more depolarized potentials as compared to other Na channels. Periods with successive null activity during pulses (hibernation) were observed. Hibernation periods became shorter with more depolarizing pulse potentials and higher hyperpolarizing holding potentials. Ensemble currents and individual records revealed two types of channel behavior: channels with apparent normal activation and inactivation kinetics, and channels that open either at the onset of or late in the pulse and stay open for prolonged periods as if both activation and inactivation were slower than that reported for other sodium channels. (Supported by NS 17928 and GM30376).

W-AM-A4 Na-DEPENDENCE AND TEMPERATURE EFFECTS ON BTX-TREATED SODIUM CHANNELS IN THE SQUID

GIANT AXON. Ana M. Correa, R. Latorre and F. Bezanilla. Department of Physiology, UCLA, Los Angeles CA; CECS, Casilla 16443 Santiago, Chile and The Marine Biological Laboratory, Woods Hole, MA.

The sodium dependence of the conductance of Na channels was studied in the presence and absence of batrachotoxin (BTX). Axons were cut open in artificial sea water and subsequently the medium was changed to 540 mM NaCl with no added Ca or Mg. Patches were formed in this solution with pipettes filled with $[Na]_i = 108$ mM, using glutamate, Cl^- and F^- as anions. The external solution was later changed to other sodium concentrations with no compensation for osmotic differences. In the BTX-treated channel, at 5°C the slope conductances were (in pS) 4.8, 5.8, 8.0, 9.6 and 10.4 for $[Na]_o$ of (in mM) 34, 135, 540, 2000, 4000 respectively. In the unmodified channel the conductances were (in pS) 16.4, 24.8 and 26.9 for $[Na]_o$ of (in mM) 540, 2000 and 4000 respectively. In $[Na]_o = 540/[Na]_i = 530$ the conductances were 9.7 and 23.6 pS for the modified and normal channels respectively. The conductance of the unmodified channel is about 2.5-fold larger than the BTX-modified channel for $[Na]_o$ of 0.5 to 4 M. The conductance is essentially invariant in the range of 0.5 to 4 M indicating that the concentration at which the channel is half saturated is much less than previously reported.

The effect of temperature on the conductance and gating properties of the BTX-modified channel was studied in the range of 5 to 23°C. In one patch with $[Na]_o = 540/[Na]_i = 530$ the conductance was 9.7 pS at 5°C and 18.3 pS at 22.3°C. In a patch with only one modified channel studied at 5 and 15°C the slope conductance showed a Q_{10} of 1.51. The kinetics of opening and closing was analyzed with models with one open state and with either one or 2 closed states and the Q_{10} varied in a wide range depending on the voltage and the particular rate constant of the transition. In the C=C=O model the average Q_{10} was 2.65. (We thank Dr. J. Daly for providing BTX. Supported by NSF INT-8610434, USPHS GM30376 and FONDECYT 1988-451).

W-AM-A5 CONDITIONS FOR NON-MONOTONIC SINGLE CHANNEL OPEN TIME DISTRIBUTIONS. L. Goldman, Dept. of Physiol., School of Med., Univ. of Maryland, Baltimore, MD. (Intr. by S. Cukierman).

Non-monotonic distributions of single channel open times (deficit of short open times, maximum at $t > 0$) were accounted for (Colquhoun and Hawkes in Single Channel Recording, pp. 135-175, 1983) with a closed, cyclic scheme including a closed and two identical open states with all transitions irreversible and proceeding in the same direction around the cycle. Such schemes require coupling to an energy source. I find neither a closed, cyclic scheme, all irreversible transitions nor coupling to an energy source are required for non-monotonic distributions. An essential requirement is that all openings are to a state from which closing is not possible, i.e. the

presence of a precursor process to closing. Consider $S_x \xrightarrow{k_{10}} S_1 \xrightarrow{k_{01}} S_0 \xrightarrow{k_{02}} S_2$ where S_x is any number of lumped closed states, S_1 and S_0 are identical open states and S_2 is a closed or an absorbing inactivated state. This is an equilibrium scheme not requiring coupling to an energy source. The open channel probability density function, is given by

$$N(t) = N_T k_{02} [-(k_{10}/a-b) \exp(-at) + (k_{10}/a-b) \exp(-bt)]$$
 with
$$a(+), b(-) = (k_{10} + k_{01} + k_{02})/2 \pm [(k_{10} - k_{01} - k_{02})/2]^2 + k_{10} \cdot k_{01}]^{1/2}$$
. N_T is the total number of openings, and is the same for openings to S_0 or S_1 . $N(t)$ is the difference of exponentials for all values of the rate constants and so always predicts a non-monotonic probability density function. There is a deficit of short open times and a maximum at $t > 0$ because there is no occupancy of S_0 at $t=0$, and some time is needed after each opening for the occupancy of S_0 to increase. Hence a non-monotonic probability density function is consistent with the presence of a precursor or kinetic delaying process. Supported by NIH grant NS07734 and by a Fulbright Senior Professor award.

W-AM-A6 THE NA INACTIVATION GATE LATCH. L. Goldman, Dept. of Physiology, School of Medicine, University of Maryland, Baltimore, Maryland 21201

Steady state to peak Na current ratio ($I_{Na\infty}/I_{Na\text{ peak}}$) in *Myxicola* giant axons is greater under some conditions in internal Cs_i than in internal K_i , i.e. less steady state inactivation develops during a step in potential in Cs_i . Cs_i effects are selective for steady state inactivation with negligible effects on the inactivation time constant (τ_h). Mean τ_h ratios (Cs_i to K_i) were 1.04 and 1.02 at 0 and 10 mV. The effect of Cs_i is to increase the fraction of inactivation gates that do not close, the rest closing normally. At the level of a single channel inactivation is blocked in an all or none manner. K_i has little effect on steady state inactivation in the presence of inward I_{Na} , with $I_{Na\infty}/I_{Na\text{ peak}}$ often declining to 0 at moderately positive potentials and independent of external Na concentration from 1/4 to 2/3 Na ASW. Cs_i also has little effect at -40 or -50 mV, but blocks inactivation more with increasingly positive potentials where single channel I_{Na} magnitude decreases. Decreasing I_{Na} by reducing external Na concentration also increases $I_{Na\infty}/I_{Na\text{ peak}}$ in Cs_i suggesting that the inactivation blocking site is located in or exposed to the Na current pathway. In K_i , $I_{Na\infty}/I_{Na\text{ peak}}$ increases on stepping from potentials where Na channel current is inward to those where it is outward, suggesting that K_i too can block inactivation in the absence of inward current. There is a site located in or near the internal mouth of the Na pore which when occupied by a cation selectively blocks inactivation gate closure. A simple explanation of these results would be that the inactivation gate normally associates with or latches to this site on closure. The inactivated state may, then, consist of a positively charged structure occluding the inner channel mouth either electrostatically or sterically if it is attached to a bulky group. (Supported by NIH grant NS 07734).

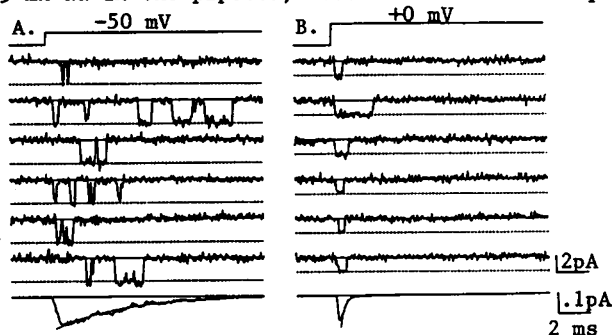
W-AM-A7 SELECTIVITY OF PURIFIED SODIUM CHANNELS FROM EEL ELECTROPLAX INCORPORATED INTO PLANAR BILAYERS IN THE PRESENCE OF VERATRIDINE. D.S. Duch, E. Recio-Pinto, S.R. Levinson and B.W. Urban. Departments of Anesthesiology and Physiology, Cornell University Medical College, New York, N.Y. 10021, and Department of Physiology, University of Colorado Health Sciences Center, Denver, Colorado 80262.

Highly purified, reconstituted sodium channels from the eel electroplax were incorporated into planar lipid bilayers in the presence of either veratridine or batrachotoxin (BTX), and their selectivity for sodium and potassium examined. Under biionic conditions (500mM NaCl outside of channels and 500 mM KCl inside, physiological orientation) reversal potentials in the presence of 50 μ M veratridine averaged 46.2 ± 1.0 mV (sem; 10 membranes), $P_{Na}/P_K=6.3$. In the reverse orientation, the average reversal potential was -51.8 ± 3.2 mV (sem; n=9 membranes), $P_{Na}/P_K=8.3$. Current-voltage relationships in symmetrical 500 mM solutions of either NaCl or KCl were linear and symmetrical. The average single channel conductances were 11.3 (NaCl) and 0.91 pS (KCl), respectively, yielding a Na:K conductance ratio of 12. For BTX-modified channels, the corresponding single channel conductances were 25 pS and 1.7 pS, respectively, with a conductance ratio of 15. Previous reversal potential measurements in 1 μ M BTX yielded a P_{Na}/P_K for these sodium channels of 4.5 (Levinson et al., 1986, Ann. N.Y. Acad. Sci., 479:162-178). It is interesting that the selectivities measured with conductance ratios are much closer to those expected for unmodified channels than the selectivities determined from reversal potential measurements.

W-AM-A8 SIMPLE GATING BEHAVIOR OF CARDIAC SODIUM CHANNELS

David T. Yue¹, John H. Lawrence, Eduardo Marban, Depts. of Biomedical Engineering¹ and Medicine (Cardiology), The Johns Hopkins University School of Medicine, Baltimore, MD 21205

Na channels from various sources demonstrate remarkably different gating properties. Those in some neural cells gate very simply, opening briefly and only once per depolarizing step; those in other preparations present a complex picture, opening multiple times before inactivating. We now report that single Na channels in guinea-pig ventricular myocytes can exhibit either simple or complicated patterns of gating, depending upon the potential of depolarizing steps. Cell-attached, unitary current records, resolved to +20 mV with 425 mM Na in the pipette, reveal that channels open very quickly, and only once per depolarization to potentials more positive than -20 mV (B). Consequently, the decay of ensemble average current tracks the dwell time of single channel openings, reminiscent of Hodgkin-Huxley kinetics. In contrast, depolarization to more negative voltages produced multiple openings before inactivation, as observed previously (A). Importantly, the observed dichotomy of gating behavior fits well with the voltage dependence of inactivation and deactivation transitions from the open state, estimated from Eyring rate theory fits to plots of mean open time vs. voltage. By analogy, differences in gating among channels from various sources could derive from subtle variations in the voltage dependence of inactivation and deactivation. These observations provide reassuring evidence for the simplest of gating subsystems surrounding the open state.



W-AM-A9 SODIUM CHANNEL ACTIVATION IN CRAYFISH GIANT AXONS: 1. MEASUREMENT OF CHANNEL VALENCE FROM SODIUM CURRENT. P.C. Ruben, J.G. Starkus and M.D. Rayner. Békésy Laboratory of Neurobiology and Department of Physiology, University of Hawaii, Honolulu, HI 96822.

The valence of sodium channel activation was determined by changing the test potential (V_{test}), holding potential (V_{hold}) or prepulse potential (V_{pre}) and measuring the peak sodium current (I_{Na}). When peak I_{Na} is plotted as a function of V_{test} (from $V_{hold}=-120$ mV), channel valence is approximately $2e^-$ when assessed either by the limiting slope method or as a Boltzmann distribution in both control axons and axons treated with pronase or chloramine-t to remove fast inactivation.

To study equilibrium properties of sodium channel activation, peak I_{Na} (at $V_{test}=+20$ mV) was measured as a function of V_{hold} (2 mins). From steady-state V_{hold} , I_{Na} shows two distinct valences: about $2e^-$ in the range from -140 mV to -90 mV, and $4-5e^-$ in the range from -90 mV to -60 mV (n=8; $p<0.0001$ by one-way analysis of variance). When 2 to 10 ms prepulses are used ($V_{hold}=-120$ mV), channel valence has a value of about $2e^-$. Longer prepulse durations show the emergence of a higher valence at V_{pre} more positive than -90 mV.

These results confirm the previous findings of Rayner and Starkus (Biophys. J., in press) suggesting that a single $2e^-$ particle is responsible for sodium channel gating current, and extend their results to show that a single such particle is sufficient to control the fast time course responses of the sodium channel. The present data further suggest that an additional "slow-inactivation" particle, with a valence of $2-3e^-$, moves in parallel to the gating particle with very slow kinetics and closes the sodium channel under equilibrium conditions. These results are consistent with a simple model of parallel sodium channel activation and slow inactivation.

Supported by PHS grant #NS21151-04, and partially from Hawaii Heart Association, UHBRSG and NIH RCMI grant RR-03061.

W-AM-A10 SODIUM CHANNEL ACTIVATION IN CRAYFISH AXONS: 2. EFFECTS OF INITIAL CONDITIONS ON THE EARLY TIME COURSE OF IONIC AND GATING CURRENTS. M.D. Rayner, J.G. Starkus and P.C. Ruben. Department of Physiology and Békésy Lab. of Neurobiology, University of Hawaii, Honolulu, HI 96822.

"Cole-Moore-type" shifts in the rising phase of I_{Na} can be demonstrated in crayfish giant axons. From intermediate holding potentials (-110 to -75 mV) hyperpolarizing and depolarizing prepulses increase or decrease respectively the "initial delay" in the rising phase of sodium current. Only hyperpolarizing prepulses affect the initial delay at holding potentials > -75 mV, whereas only depolarizing prepulses are effective from strongly negative holding potentials. Such shifts reach their full magnitude within about the first $100 \mu s$ of the prepulse, thereafter remaining constant with further increases in prepulse duration (cf Hahn and Goldman J.G.P.80:83-102).

Although lateral shifts are also evident in the falling phase of gating current (see Taylor and Bezanilla, 1983, J.G.P.81:773-784), we find that these shifts do not saturate at $100 \mu s$, increasing continuously with increases in prepulse duration. In crayfish axons, the observed changes in I_g waveform arise in part from changes in the intercept (but not the kinetics) of the intermediate and slow I_g components, and in part from kinetic changes within the fast I_g component. None of these changes appear directly related to the "Cole-Moore-type" shifts seen in the rising phase of I_{Na} .

We conclude that opening of the sodium channel involves transit through intermediate preopen states. By contrast no clear evidence exists for equivalent intermediate states in gating current. These results are consistent with a model in which a voltage sensitive gating particle interacts electrostatically with a relatively voltage insensitive activation gate (with two preopen positions).

Supported by PHS grant #NS21151-04, and partially from Hawaii Heart Association, UHBRSG and NIH RCMI grant RR-03061.

W-AM-B1 DIFFERENCES IN THE CALCIUM SENSITIVITY AND ENDPLATE CHANNELS EXPRESSED BY SNAKE TONIC AND TWITCH MUSCLE FIBERS by R.L. Ruff, Neurology Dept. Cleveland VA Medical Center and Case Western Reserve University School of Medicine, Cleveland Ohio 44106

Garter snake costocutaneous muscles are composed of singly-innervated twitch muscle fibers that have en plaque endplates, and multiply-innervated tonic muscle fibers which have simple en grappe synapses. The ACh receptor (AChR) channels found in the endplate of twitch and tonic fibers from garter snake costocutaneous muscle fibers were studied by enzymatically removing the nerve terminal and performing patch-clamp recordings on the exposed postsynaptic membrane. The endplates from twitch fibers had only one class of endplate channel with a conductance of about 51 pS in physiological snake saline and a mean open channel duration of 3.59 ms. The endplates of tonic fibers had two types of channels. One AChR channel in the tonic fibers resembled the type seen in twitch fibers with a conductance of 51 pS and a channel duration of 3.51 ms. The other channel in tonic fibers had a smaller conductance of 33 pS. The channel open-time histogram of the small conductance channel was best fit by a double gaussian curve with means of 1.22 ms and 7.55 ms. The ratio of the conductances of the small and large conductance channels in tonic fibers was similar to that previously found for fetal-type and adult-type AChRs in mammalian skeletal muscle.

Snake costocutaneous muscle fibers were chemically skinned and Nomarski optics was used to identify individual tonic and twitch fibers based upon the morphology of the endplate region. The normalized tension generated by the two types of fibers were similar, but they had very different calcium sensitivities. The twitch fibers generated tension over a narrow range of calcium concentrations. The tonic fibers had lower threshold calcium concentrations for tension generation and had a 10 fold larger range of calcium concentrations between threshold and maximum tension.

The differences in the single fiber properties between tonic and twitch snake muscle fibers may permit these fibers to perform different motor tasks.

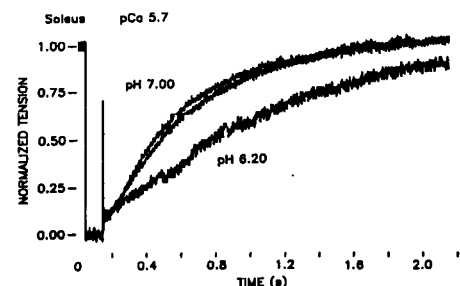
Supported by Merit Reviewed funding from the Veterans Administration.

W-AM-B2 CA-DEPENDENCE OF A MYOSIN HEAVY CHAIN (HC) PEPTIDE BINDING TO AND DISSOCIATION FROM SKINNED FIBERS FROM RABBIT PSOAS MUSCLE. P.B. Chase and M.J. Kushmerick, Dept. of Radiology, Univ. of Washington, Seattle, WA 98195.

The 7 amino acid synthetic peptide (sequence IRICRKG--the same as myosin HC around SH₁) binds to pure F-actin and inhibits actin-S1 rigor complex formation (Suzuki et al., 1987, JBC 262:11410). In addition to its effects *in vitro*, it also inhibits maximum Ca-activated force in skinned psoas muscle fibers (Chase and Kushmerick, 1989, FASEB J., in press) but does not alter the force-pCa relation (peptide $1.2 \times K_D$). Force development and relaxation are faster (seconds) than peptide effects on force (minutes); thus brief activations can be used to assay for peptide binding in the absence of Ca²⁺. Pre-incubation with peptide ($5 \times K_D$) at pCa > 8 results in little or no force inhibition during a test activation (pCa 4.5) with no peptide. Force developed at pCa 4.5 in the presence of peptide ($5 \times K_D$) was $8.3 \pm 1.4\%$ of that without peptide; changing the solution to an activating solution with no peptide results in force recovery to the control level, with > 50% recovery in 10 min. If, after an activation in the presence of peptide the fiber is relaxed (pCa > 8) with no peptide, there is no force recovery after 10 min when assayed by a brief activation (pCa 4.5, no peptide). These results suggest that myosin HC peptide IRICRKG has functionally significant interactions only with the thin filaments of skinned fibers and that peptide binding to native actin filaments is regulated by Ca²⁺. The results are consistent with a model of Ca-induced structural changes on the thin filament which, upon removal of Ca²⁺, (1) block the peptide's binding site on actin and (2) trap previously bound peptide. Supported by NIH grant AM36281 and by NIH fellowship AM07783 to PBC.

W-AM-B3 VARIATIONS IN CALCIUM SENSITIVE CROSS-BRIDGE ATTACHMENT RATE DUE TO ALTERED pH IN FAST- AND SLOW-TWITCH SKINNED SINGLE SKELETAL MUSCLE FIBERS. Joseph M. Metzger and Richard L. Moss. Department of Physiology, University of Wisconsin, Madison, WI 53706.

Under conditions of sarcomere length control, Ca²⁺ sensitive increases in the rate constant of tension redevelopment (k_{tr}) following step release and re-extension of muscle length have been related to increases in f , the rate constant of cross-bridge attachment in A.F. Huxley's model of contraction (Brenner PNAS 85:3265, 1988). In the present study the Ca²⁺ sensitivity of k_{tr} was examined at a control pH of 7.00 and at pH 6.20, the value achieved in muscle cells during intense contractile activity. At high concentrations of Ca²⁺ (pCa 4.5 to 5.5), k_{tr} was unaffected by reducing pH from 7.00 to 6.20 in slow and fast fibers. However, at lower concentrations of Ca²⁺ (pCa 5.7 to 6.0) k_{tr} was significantly depressed upon reducing pH to 6.20 (Figure). In this example, the $t_{1/2}$ for tension redevelopment increased from a value of 315 ms at pH 7.00 to 693 ms at pH 6.20. The effect of pH to depress k_{tr} was completely reversed by returning pH to 7.00. In contrast to k_{tr} , isometric tension was depressed throughout the entire range of pCa's (pCa 4.5 to 6.0), thus demonstrating dissociation of steady state tension development and k_{tr} . H⁺ ion mediated reductions in the Ca²⁺ sensitivity of f may provide a molecular basis for reduced dP/dt during fatigue. Supported by NIH.



W-AM-B4 EFFECT OF Ca^{++} -ACTIVATION UPON FORCE-VELOCITY-RELATION. FURTHER EVIDENCE FOR Ca^{++} -REGULATION AFFECTING CROSS-BRIDGE TURNOVER KINETICS.

B. Brenner. Institute of Physiology II, University of Tübingen, D-7400 Tübingen, FRG.

We previously showed that the rate constant of force redevelopment (k_{redev}) subsequent to a period of isotonic shortening and rapid restretch to the original overlap is sensitive to the level of Ca^{++} -activation (Brenner, PNAS 85, 3265, 1988). Assuming that force redevelopment reflects the reapproach of the isometric steady state distribution of cross-bridges between weak and strong binding states (Brenner, BRC 81, 1, 54, 1986), this finding was interpreted to suggest that Ca^{++} -activation modulates cross-bridge turnover kinetics, specifically $f_{app} + g_{app}$, where f_{app} characterises the transition from the weak to the strong binding states while g_{app} determines the return back to the weak binding states via ADP-release and rebinding of ATP. Since this interpretation depends upon the assumption that k_{redev} mainly reflects $f_{app} + g_{app}$ while other factors (e.g., changes in activation level due to the experimental procedure) are insignificant, we now studied the effect of Ca^{++} -activation upon the curvature of the force-velocity-relation. According to the theory of Huxley (Prog. Biophys. 7, 255, 1957), this curvature is another parameter dependent upon cross-bridge turnover kinetics. Using our previously proposed method for determining shortening velocity (Brenner, JMRCM 1, 409, 1980; BRC 81, 54, 1986), we find the curvature of the force-velocity-relation to change with Ca^{++} -activation while, as in our previous work (Brenner, 1980, 1986), maximum unloaded shortening velocity (v_{max}) is not significantly affected. Interpretation of these results on the basis of Huxley's theory (1957) again suggests a change in $f_{app} + g_{app}$ with Ca^{++} -activation while g_0 , as probed by v_{max} , remains unchanged. Supported by DFG Br 849/1-2. Present address: Abtl. f. Allg. Physiologie, Universität Ulm, Oberer Eselsberg, D-7900 Ulm, FRG.

W-AM-B5 HYSTERESIS, AND THE LENGTH DEPENDENCE OF Ca^{2+} -SENSITIVITY, IN MUSCLE WITH CARDIAC TnC EXCHANGE: FURTHER INSIGHTS INTO THE MECHANISM OF STARLING'S LAW OF THE HEART.

J. Gulati and A. Babu, Albert Einstein College of Medicine, Bronx, NY 10461.

Exchanging cardiac (C) TnC with skeletal (S) TnC reduces the length dependence of Ca^{2+} -sensitivity in cardiac muscle, suggesting that CTnC itself is the long sought length transducer in the Starling's law of the heart (Babu et al, Science, 240, 74, 1988). A critical test of this hypothesis is made here by studying whether the converse CTnC-for-STnC exchange enhances the length-dependence in skeletal muscle. In addition, since hysteresis in the force- Ca^{2+} relation (Ridgway and Gordon, Science, 219, 1075, 1983) indicates length dependence too (Harrison et al, J Physiol, 401, 115, 1988), we studied the effect of TnC exchange to compare the mechanisms of hysteresis and Starling's law. CTnC-loaded fast-twitch fiber from rabbit psoas gave full force with maximal $[Ca^{2+}]$ in 100nM salt at 5°C. In fibers with STnC, the Ca^{2+} -sensitivity was decreased by $0.15 \pm .01$ (5) pCa unit with change in sarcomere length from 2.4µm to 1.9µm. After CTnC exchange, the length induced shift in sensitivity was increased to $0.26 \pm .02$ (4) pCa unit, which confirms the original hypothesis. Further, partially extracted fibers had the same length dependence as native fibers. The TnC levels were checked with silver stained gels. Hysteresis was $0.09 \pm .01$ on 5 fibers with STnC, and $0.08 \pm .01$ (6) with CTnC. We conclude that 1) CTnC is a better length transducer than STnC in myocardial and skeletal milieus. 2) The length effect on Ca^{2+} -sensitivity is independent of cross bridge number. And 3) the molecular basis of hysteresis is separate from the mechanism underlying Starling's law. [Supported by NIH, and NY Heart Association.]

W-AM-B6 IS THE MECHANICS OF INSECT LEG MUSCLE MORE LIKE THAT OF ASYNCHRONOUS INSECT FLIGHT MUSCLE OR VERTEBRATE (RABBIT PSOAS) MUSCLE? J.E. Molloy, M. Peckham, J.C. Sparrow and D.C.S. White. Department of Biology, University of York, YO1 5DD, U.K.

Rabbit psoas muscle is fully activated by calcium and, once activated, has a small non-maintained delayed tension increase in response to a small rapid stretch. In contrast, asynchronous insect flight muscle (IFM) is partially activated by calcium and has a large maintained delayed tension increase in response to stretch. We have compared the mechanical properties of single IFM and leg glycerinated muscle fibres from *Lethocerus indicus* and *Drosophila melanogaster* (leg muscle was Tergor Depressor Trochantor (TDT)). We found that the mechanics of leg muscles were more like that of rabbit psoas than IFM; they were fully activated by calcium and they had a small, poorly-maintained delayed tension in response to a stretch. However, the rate constant for the delayed tension increase was similar to that of IFM. Full activation by calcium is consistent with the high sarcoplasmic reticulum content of both rabbit psoas and TDT. IFM is different to rabbit psoas muscle in several other ways; it has short I-bands and a high relaxed stiffness, it has oscillation activation of the ATPase in active muscle, and it has both a simple pathway for oxygen exchange and a matching periodicity of the A- and I-filament helices (38.5nm). Present studies of the effect of a single mutation of a contractile protein on the properties of *Drosophila* IFM (see Sparrow et al, this meeting) can now be extended to look at possible different effects of expression of the same muscle mutations in both TDT and IFM.

W-AM-B7 TENSION TRANSIENT DURING SLOW LENGTHENING OF FROG MUSCLE FIBRES. F. Colomo, V. Lombardi and G. Piazzesi (Intr. by G. Cecchi). Dipartimento di Scienze Fisiologiche, Università degli Studi di Firenze, 50134 Firenze, Italy.

Tension transients (Huxley and Simmons, *Nature* 233:533-538, 1971) were elicited at the isometric tetanus plateau (T_0) or at a time during lengthenings at low velocity (0.07-0.09 $\mu\text{m/s}$ per half-sarcomere, h.s.) when tension had attained a steady level (1.6-1.7 T_0), by imposing step releases complete in 110 μs to single fibres isolated from the tibialis anterior muscle of the frog. Experiments were performed at 3-5 °C and at about 2.1 μm sarcomere length. The actual length changes of a short tendon-free fibre segment selected along were measured by means of a "striation follower" (Huxley et al. *J. Physiol.* 317:12-13P, 1981). The linear part of the T_1 relation determined at T_0 extrapolated to zero tension at 4 nm per h.s. For the same fibres as above even if the T_1 relation was steeper during lengthening than under isometric conditions, its linear part extrapolated to zero tension at 5.3 nm per h.s. The value of Y_0 was, therefore, 32.5 % larger during lengthening than at T_0 . During lengthening the amount of tension recovery during phase 2 was smaller than at the isometric plateau for small releases and greater for large ones, so that the length axis intercept of T_2 relation was shifted to the left by about 3 nm per h.s.

In terms of the theory of Huxley and Simmons (1971) these results imply that slow lengthening of active muscle causes not only an increase in the average force per cross-bridge but also a redistribution of attached cross-bridges towards a low force generating state.

W-AM-B8 PASSIVE VISCOELASTIC PROPERTIES OF RAPIDLY EXTENDING SINGLE MUSCLE FIBERS. E.Meyhofer and T.L.Daniel (Intr. M.M. Bosma). Dept of Zoology, Univ. Washington, Seattle WA 98195.

The mechanical properties of muscle are assumed to be dominated by passive elastic elements in series with contractile elements. But nearly all tissues are viscoelastic, and the extent to which viscosity may contribute to the mechanical properties of muscle fibers is unknown. To study this problem we chose a model system: large extensor fibers from the shrimp, *Pandalus danae*, which are rapidly extended (~30 ms) during the animal's escape response. Such high rates of length change may greatly enhance the effect of viscosity on the mechanical response of the cell. Two fiber types were studied: large medial extensors and smaller adjacent ones. All fibers were mechanically dissected, chemically skinned and completely relaxed. Force measurements of cells exposed to sinusoidal length changes over a range of frequencies and sarcomere lengths (0.5-120 hz; 1.9-3.2 μm) were used to determine the elasticity and viscosity. Results show that these fibers are indeed viscoelastic with viscous and elastic moduli of similar magnitudes. All moduli increase weakly (two fold) with frequency and strongly (ten fold) with sarcomere length over the range tested. The ratio of viscous to elastic moduli decreases slightly with increasing sarcomere length and ranges from 0.25 - 0.5. Interestingly, this ratio also shows a non-monotonic frequency dependence with a maximum ratio of about 0.5 at 60 hz for large fibers and about 100 hz for small fibers. The physiological loading frequency is about 60 hz. From these data we conclude that the viscous component is large and cannot be neglected in analyses of mechanical behavior: about half of the mechanical energy imparted to fibers in each cycle of loading is passively dissipated. The relative energy dissipation is largest in the middle of the physiological range, indicating that the fibers are maximizing viscous losses. We hypothesize that such high viscosity maintains a stable response to rapid length change, since purely elastic system with mass may respond unstably to time-varying loads.

W-AM-B9 EFFECT OF ACTIVE PRE-SHORTENING ON ISOMETRIC AND ISOTONIC PERFORMANCE OF SINGLE FROG FIBERS. Henk L. Granzier* and G.H. Pollack. Division of Bioengineering WD-12, University of Washington, Seattle, Wa 98195.

*Present address: Department of Chemistry, University of Texas at Austin, Austin, TX, 78712

According to the cross-bridge model, maximal isometric force is determined by the instantaneous degree of overlap, not by the degree of overlap when contraction started. However, it is well documented that reducing overlap by stretching tetanized fibers results in more force than predicted; force is enhanced. On the other hand, the effect of increasing overlap by imposing shortening is less clear. We investigated this issue.

The effects of shortening history on isometric force and isotonic velocity were studied by first tetanizing fibers isometrically and when force reached a plateau, shortening was imposed, after which the fiber was held isometric again. Isometric force after shortening could then be compared with controls in which no shortening had taken place.

Sarcomere length was measured simultaneously with two independent methods: a laser-diffraction method and a segment-length method. The fiber was mounted between two servomotors. One was used to impose the load clamp while the other cancelled the translation that occurred during this load clamp. Thus, translation of the segment under investigation could be minimized.

Isometric force was unaffected by previous sarcomere shortening provided the shortening occurred against either a low load or over a short distance. However, if the work done during shortening was high, force after shortening was less than if sarcomeres had remained at the final length throughout contraction. The correlation between the force deficit and the work done during shortening was statistically significant ($p=0.0001$).

Interrupting the tetanus for 0.5-3.0 seconds did not reverse the effects of shortening on isometric force; at least 5-10 minutes of rest were required before force recovered completely.

Sarcomeres accelerated during the period of shortening under constant load, indicating that the sarcomeres became progressively stronger. However, the acceleration was less than that predicted from the force-velocity relation applicable at each of the sarcomere lengths transversed during shortening. Velocity of shortening appeared to be much more sensitive to previous shortening than isometric force.

Results obtained with the diffraction method were the same as those obtained with the segment length method. Therefore, it is unlikely that heterogeneous behavior of sarcomeres within the sampled region underlies any of the observed effects. Explanations for the deficit in contractile performance will be discussed.

W-AM-B10 FORCE-LENGTH RELATIONS OF "ALMOST ISOMETRIC" SARCOMERES. Arie Horowitz, Casper J. Caljouw and Gerald H. Pollack, Center for Bioengineering WD-12, University of Washington, Seattle WA 98195.

Force-length relations measured in several laboratories (Gordon *et al.*, 1966; Edman and Reggiani, 1987) as well as in this laboratory (see relevant poster by Granzier and Pollack) were found to have a linear descending limb; but in other studies, the force-length curve was flatter and nonlinear (Fabiato and Fabiato, 1978; ter Keurs *et al.*, 1978; Tameyasu *et al.*, 1983). A possible reason for the difference is that in the first type of experiment, a length clamp was used to keep sarcomeres strictly isometric. In the second type, however, limited sarcomere shortening was not excluded. If force generation is assumed to be accompanied by measurable mechanical work, and hence, by sarcomere shortening, absolutely isometric sarcomeres (which perform no mechanical work) could conceivably be merely force sustainers. Thus, the length-clamp protocol might measure tension sustenance, while the other one measures tension-generation. We tested this hypothesis. Single skeletal fibers were tetanized under isometric conditions and sarcomere length was acquired on line by laser diffraction. The intensity profile of the first order was recorded throughout the contraction in order to check for homogeneity of the observed sarcomere group; relatively small dispersion was found. Markers placed on the fibers within the field of observation typically translated only by about 10 microns during the plateau phase of the tetanus; hence, the same sarcomere group was followed during the contraction. At least one sarcomere group that underwent continuous and very limited shortening (less than 3%) during the plateau phase could be found in each fiber. In these sarcomeres, deactivation and velocity effects are negligible due to the small amount of shortening. The resulting force-length curve of these nearly isometric sarcomeres was found to be almost flat up to a sarcomere length of 3.0 microns. Thus, slightly shortening, force-generating sarcomeres undergo a smaller decline in force at longer lengths than purely isometric ones.

W-AM-B11 MYOSIN SHORTENING EXPLAINS FORCE DEVELOPMENT BEYOND OVERLAP IN SKINNED SKELETAL GRACILIS MUSCLE OF THE RABBIT. Evert L de Beer, Rob LF Grundeman, Anneke *Veenendaal, Karel JH van **Buuren, Piet Schiereck. Depts. Med. Physiol., *Cell Biol. and **Pharmacol. University of Utrecht, Vondellaan 24, 3521 GG Utrecht, The Netherlands.

Force development beyond overlap has been ascribed to artefacts such as passive shortening of long sarcomeres (> 3.6 μm) by active short sarcomeres (< 3.6 μm) (Julian & Moss, 1980, J. Physiol. 304:529). In order to investigate this possibility quantitatively, we performed two protocols on one and the same fiber at an initial length of 4.0 μm (measured by means of laser diffraction): I) A stretch of the passive fiber, thereby measuring the induced force and length transients. II) Activation of the fiber and measuring the induced force and sarcomere changes.

From protocol I we estimated the fraction of force due to passive stretch of the long sarcomeres as observed in protocol II. The highest observed contribution of force observed in protocol II induced of passive stretch was 40%. Typical values were less than 10%.

Electron micrographs obtained from fibers directly fixated after the experiment in the relaxing or activating bathing solutions reveal a shortening of the myosin filament from 1.62 to 1.42 μm due to activation. Assuming: A) The passive stiffness of the muscle is located in connectin (Horowitz & Podolsky, 1988, Biophys. J. 54:165) and is measured in protocol I; B) Shortening of myosin induces stretching of connectin, then we can calculate the induced force in the connectin filament during activation. This calculated value agrees (within the experimental error) with the observed force.

This study was supported by The Netherlands Organization of Scientific Research (NWO).

W-AM-B12 EFFECT OF MYOSIN LIGHT CHAIN PHOSPHORYLATION ON MECHANICAL AND BIOCHEMICAL PROPERTIES OF SKELETAL MUSCLE FIBERS. H.L. Sweeney and J.T. Stull, Univ. of Texas at Austin, Texas, 78712, and Univ. of Texas Southwestern Medical Center at Dallas, Texas, 75235.

We have examined the effect of myosin light chain phosphorylation on force, stiffness, isometric ATPase activity, and the rate constant for force redevelopment in permeabilized rabbit psoas fibers at 15° C. These measurements were made over a range of calcium concentrations that produced between 10 and 50% of maximal isometric force. Myosin light chain phosphorylation in control fibers was 10% or less whereas preincubation with purified myosin light chain kinase and calmodulin at pCa 5.4 resulted in 80% phosphorylation. Myosin light chain phosphorylation resulted in a leftward shift of the pCa-force relationship over this range of calcium concentrations, as previously demonstrated (Sweeney and Stull, AJP 250:C657-660, 1986). The rate constant for force redevelopment increased with light chain phosphorylation and showed a similar leftward shift with pCa. The isometric ATPase activity increased with phosphorylation and was linearly proportional to the increase in force. Likewise the increase in fiber stiffness was proportional to the increase in force. Following the types of analyses described by Brenner (PNAS 85: 3265-3269, 1988), we used the force, stiffness, ATPase, and force redevelopment data to determine the effect of myosin light chain phosphorylation on the rate constants characterizing the transitions to force-generating states (f_{app}) from nonforce-generating states (g_{app}) and the reverse. The data showed that phosphorylation of myosin light chain increased f_{app} but had no effect on g_{app} . This implies that myosin phosphorylation does not make more cross-bridges available for actin binding at low calcium concentrations, but increases the probability of cross-bridges entering the force producing state. The lack of effect on g_{app} is consistent with previous observations that myosin light chain phosphorylation does not change the maximal shortening velocity. (Supported in part by HL06296.)

W-AM-C1 CAFFEINE ACTIVATES CALCIUM-INDUCED CALCIUM RELEASE IN VOLTAGE-CLAMPED SKELETAL MUSCLE FIBERS. B.J. Simon, M.G. Klein and M.F. Schneider. Dept. of Biological Chemistry, Univ. of Maryland School of Medicine, Baltimore, MD 21201.

Myoplasmic $[Ca^{2+}]$ was monitored simultaneously by fura-2 and antipyrylazo III in cut frog skeletal muscle fibers voltage-clamped to -100 mV in a double Vaseline gap ($8-10$ °C). Caffeine (0.5 mM) increased the amplitude of the $[Ca^{2+}]$ transient ($\Delta[Ca^{2+}]$) during all pulses and slowed the decline of $\Delta[Ca^{2+}]$ after all pulses. In control $\Delta[Ca^{2+}]$ began to decline sharply 2-4 ms after repolarization. In 0.5 mM caffeine $\Delta[Ca^{2+}]$ continued to rise for up to 45 ms following 10-20 ms pulses, demonstrating that calcium release from the SR continued for at least that long after repolarization in caffeine. This loss of fiber membrane potential control of release was likely due to caffeine-activated $[Ca^{2+}]$ -induced calcium release. Following longer (60-200 ms) pulses $\Delta[Ca^{2+}]$ began to decline within a few ms of repolarization even in caffeine, indicating an inactivation of the caffeine-activated $[Ca^{2+}]$ -induced release. Records of the rate of release (R_{rel}) of calcium calculated from $\Delta[Ca^{2+}]$ were increased in 0.5 mM caffeine. During long pulses R_{rel} in caffeine declined toward a steady level with the same time constant as without caffeine, indicating that both inactivated by the same $[Ca^{2+}]$ -dependent process (J. Physiol., 405:727, 88). Release after short pulses in caffeine declined to zero with the same time constant, indicating that this turn off was by release inactivation rather than by release deactivation at repolarization as in control. Caffeine caused no change in charge movement during or after pulses. Caffeine appears to activate a $[Ca^{2+}]$ -induced calcium release that continues after short pulses and inactivates similarly to release in the absence of caffeine.

W-AM-C2 EFFECTS OF CAFFEINE AND PROCAINE ON CALCIUM RELEASE IN VOLTAGE-CLAMPED SKELETAL MUSCLE FIBERS. M.G. Klein, M.F. Schneider and B.J. Simon, Dept. Biological Chemistry, Univ. of Maryland School of Medicine, Baltimore, MD 21201.

The rate of release (R_{rel}) of calcium from the SR during 60-200 ms depolarizing pulses was calculated from measured $[Ca^{2+}]$ transients (Simon et al, 89, these abstracts) and was corrected for calcium depletion from the SR. Release calculations in caffeine and/or procaine assumed calcium removal and SR calcium content to be the same as control. In all cases R_{rel} reached an early peak and then declined to a steady level. Caffeine (0.5 mM) shifted the voltage dependence of peak (-8.1 ± 1.2 mV; mean \pm se, $n = 5$) and steady level (-8.7 ± 2.2 mV) to more negative potentials with little change in steepness, and increased the maximum peak ($27 \pm 9\%$) and maximum steady level ($15 \pm 13\%$). These effects could be due to $[Ca^{2+}]$ -induced calcium release activated by caffeine (Simon et al, 89). 0.3 mM procaine added to fibers in 0.5 mM caffeine largely suppressed the continued release seen after short pulses in caffeine (Simon et al, 89) while 1 mM completely blocked the effect of caffeine. Without caffeine 0.3 mM procaine had no effect while 1 mM procaine scaled down the peak and steady release by $34 \pm 4\%$ and $37 \pm 12\%$ ($n=3$) without altering the voltage dependence. Resting $[Ca^{2+}]$ increased 22% in caffeine and decreased 12% in 1 mM procaine. Neither drug altered intra-membrane charge movement. Possible Interpretations: (1) 0.3 mM procaine blocked the $[Ca^{2+}]$ -induced release activated by 0.5 mM caffeine whereas 1 mM procaine partially suppressed $[Ca^{2+}]$ -independent release in control, or (2) procaine blocked only $[Ca^{2+}]$ -induced release and the releases in both the presence and absence of caffeine were $[Ca^{2+}]$ -induced but were more sensitive to procaine in caffeine.

W-AM-C3 DIFFERENTIAL INHIBITION OF Ca^{2+} -DEPENDENT AND Ca^{2+} -INSENSITIVE ^{45}Ca RELEASE IN SKINNED MUSCLE FIBERS. E.W. Stephenson, Dept. of Physiology, UMD-NJ Medical School, Newark, NJ 07103.

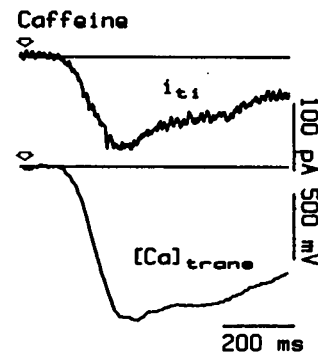
Depolarizing ion gradients stimulate mechanically skinned fibers to release ^{45}Ca with a large Ca^{2+} -dependent and small Ca^{2+} -insensitive component (J. Gen. Physiol. 86:813, 1985; in press). Selective inhibition of this stimulus in highly stretched fibers (J. Gen. Physiol. 88:56a, 1986; in press) supports other evidence that it is T tubule mediated. The present studies show that the stretch effect is reversible, inhibition increases with the rate of stretch, and the Ca^{2+} -insensitive component is unaffected. Skinned segments of frog semitendinosus fibers, loaded with ^{45}Ca and rinsed at sarcomere length (SL) 2.3 μ m, were stimulated by choline Cl/K methanesulfonate replacement (constant $[K^+][Cl^-]$, 5 mM MgATP) at either 2.3 μ m SL or twice the length at which SL was 2.2 μ m. a) Segments stretched and returned to normal SL before ^{45}Ca loading and Ca^{2+} -dependent stimulation (preceding EGTA addition) released the same ^{45}Ca (35.6% , (4)) as unstretched segments from the same muscles (36.2% (5)). b) In 9 segments stretched after ^{45}Ca loading and before Ca^{2+} -dependent stimulation, ^{45}Ca loss relative to that in paired unstretched segments from the same fiber was inversely (linearly) correlated with the rate of stretch ($r = 0.8292$, $P < 0.01$). c) In segments stretched after ^{45}Ca loading and before stimulation in the presence of 5 mM EGTA, Ca^{2+} -insensitive ^{45}Ca release remained significantly above unstimulated loss in paired segments from the same fiber, $+2.13 \pm 0.34\%$ (7), did not differ from that in paired unstretched segments from the same fiber, and was not correlated with stretch rate. These results are consistent with the hypothesis that the Ca^{2+} -insensitive component reflects intermediate coupling steps associated with the T tubule. [Supported by NIH grants AM 30420 and 2 S07 RR05393].

W-AM-C4 MALIGNANT HYPERTHERMIA AFFECTS GATING OF CALCIUM RELEASE CHANNELS. J. Vilven, J.R. Mickelson, B.A. Jacobson, C.F. Louis, and R. Coronado. Department of Physiology and Molecular Biophysics, Baylor College of Medicine, Houston, TX and Department of Veterinary Biology, University of Minnesota, St. Paul, MN.

The nature of the defect in the Malignant Hyperthermia Syndrome was examined in native sarcoplasmic reticulum (SR) vesicles from a porcine model incorporated into planar bilayers. To avoid the use of large divalent concentrations to measure current, we used CsCl as the current carrier. This permitted us to study the Ca dependence of the release channel at physiological Ca levels (Fill et al., 1988, submitted). Cs also was helpful in blocking SR K channels which comprise a significant fraction of the background conductance of the SR. At pH 7.4, pCa 6, release channels from normal and MHS have a conductance of approximately 460 pS and 440 pS, respectively which is the same reported by Smith et al. in the purified ryanodine receptor from rabbit skeletal muscle in the same solutions (250 mM/50 mM CsCl; JGP 92:1-26, 1988). At pH 7.4, pCa 6, HPs from 0 mV to +50 mV, decreased open probability from $p=0.8$ to $p=0.05$ in the MHS channel but not in the normal release channel. In normal and MHS, channels are closed to $p<0.01$ at pH 6.8. In MH but not in normal, a drop in pH from 7.4 to pH 7.0 is accompanied by a severe time-dependent and voltage-dependent inactivation whereby channels do not open at +30 mV or more positive without a prepulse to 0 mV. Evidently, the kinetics of release channels is grossly altered in MHS. Supported by NIH, MDA, and AHA.

W-AM-C5 CAFFEINE-INDUCED Ca^{2+} RELEASE STIMULATES EFFLUX OF Ca^{2+} VIA THE Na^+-Ca^{2+} EXCHANGER IN SINGLE MAMMALIAN CARDIAC MYOCYTES. G. Callewaert, L. Cleemann and M. Morad. Department of Physiology, University of Pennsylvania, Philadelphia, PA 19104.

Caffeine is known to release Ca^{2+} from, and impair its reuptake into the sarcoplasmic reticulum of skinned or intact muscle preparations. Caffeine is also known to induce a transient inward current (i_{ti}) in atrial 'cardioballs' (Mechmann & Pott (1986), Nature 319, 597) and embryonic heart cells (Clusin et al. (1983), Am.J.Physiol. 245, H528). We have used the Ca^{2+} -indicator dye fura-2 dialyzed into rat and guinea-pig ventricular myocytes in order to measure directly the relationship between i_{ti} and the intracellular Ca^{2+} -transient ($[Ca]_{trans}$) evoked by rapid (<50 ms) application of 0.5-5 mM caffeine. i_{ti} activated with the same time course as the $[Ca]_{trans}$ (see fig.) and its magnitude was directly correlated to the amplitude of the $[Ca]_{trans}$. 3 mM Ni^{2+} or Na^+ -free solution suppressed i_{ti} but had little effect on the $[Ca]_{trans}$. The magnitude of i_{ti} (50-200 pA, $t_{1/2} = 2-5$ s) was sufficient to correspond to removal of a noticeable fraction of the intracellular Ca^{2+} . We conclude that the caffeine-induced i_{ti} represent efflux of Ca^{2+} via the Na^+Ca^{2+} exchanger. Supported by NIH grants HL16152 and HL33720.



W-AM-C6 DEPOLARIZATION RAISES INTRACELLULAR pH (pH_i) IN ACID-LOADED FROG MUSCLE, EVEN THOUGH IT LOWERS IT IN NORMAL MUSCLE. C. Amorena, J.K. Manchester*, T.J. Wilding and A. Roos. Dept. of Cell Biol. and Physiol. and Dept. of Pharmacol.*, Washington Univ. Sch. of Med., St. Louis, MO 63110.

When the superfusate ($\emptyset CO_2$, $\emptyset Na$, 10 mM HEPES, pH_o 7.35) of frog semitendinosus was changed from 2.5K to 25K, pH_i measured with liquid membrane microelectrodes gradually fell by $.24 \pm .06$ from $7.35 \pm .06$ (SEM, $n=11$). However, after acid loading to pH_i $6.36 \pm .03$ (9) by a 20 mM NH_4Cl prepulse, 25K rapidly raised pH_i by $.35 \pm .06$. In both cases V_m^i fell from ~ -85 to ~ -55 mV. Caffeine (1 mM) at low pH_i (2.5K) also raised pH_i . These rises were blocked by tetracaine (.2 mM). Reducing pH_o of the acidic muscle by 1 unit had no effect on the 25 K-induced pH_i rise, but 2,4-dinitrofluorobenzene (which inactivates creatine phosphokinase) abolished it; there was no effect at normal pH_o . ATP and phosphocreatine (PCr) were assayed at 2.5 and 25K in 93 fibers of 26 paired bundles frozen with cooled freon. ATP was about the same in all fibers (av. of the groups 21.1-25.1 mmol/Kg dry wt.). PCr at 2.5K was nearly the same at normal pH_i (144 mmol/Kg dry wt.) and after pH_i had been lowered to ~ 6.0 (124). However, PCr was reduced by 53% in the 5 acid-loaded bundles frozen near peak of 25K-induced alkalinization (pH_i rise $.28 \pm .05$ from $6.21 \pm .05$). At normal pH_i PCr remained unchanged in 5 bundles after the same period (~ 7 min) in 25K but was 35% lower (3 bundles) after ~ 16 min. The 25K- or caffeine-induced pH_i rise in acid-loaded muscles is interpreted as due to Ca release-initiated PCr breakdown needed to maintain ATP in the face of the known inhibition of glycolysis by acidity. When Ca is released at normal pH_i , PCr initially is apparently not required to maintain ATP. Later, PCr breakdown would minimize acidification. Supported by NIH Grants HL 00082 (to A.R.) and NS 08862 (to J.K.M.).

W-AM-C7 SR Calcium-Induced Calcium Release Channels are Likely to be Involved in Excitation-Contraction Coupling in Vertebrate Skeletal Muscle. D.G. Brunder and P.T. Palade, Department of Physiology and Biophysics, University of Texas Medical Branch, Galveston, TX 77550.

Calcium-induced calcium release has been proposed as a mechanism for excitation-contraction coupling (Endo *et al.*, *Nature* 228:34, 1970). Previously (Biophys. J. 53:602a, 1988) we have shown that calcium release from *in vitro* SR vesicle preparations is more sensitive to inhibitors of calcium-induced calcium release than is e-c coupling in single voltage-clamped frog skeletal muscle fibers. We have extended these studies to determine the effect of putative inhibitors on the ability of caffeine to potentiate Ca release from SR of TTX-treated single frog muscle fibers in a Hille-Campbell vaseline gap voltage clamp. Ca release is estimated from: 1) the shortest stimulus to +100 mV (from the holding potential of -90 mV) that just elicits a local contraction of the fiber; and 2) direct measurement of Ca²⁺ transients with Antipyrilazo III. We have applied various concentrations of gentamicin, neomycin, ruthenium red, spermine, and protamine to the cut ends of voltage clamped fibers and determined the degree of inhibition of SR calcium release. The amount of inhibition of calcium release by a drug is highly correlated with the drug's effect on caffeine (0.5 mM) potentiation of the SR calcium release. This suggests that the same channels which are opened by caffeine participate in e-c coupling, and that *in vitro* studies under non-physiologic conditions do not always reflect drug effects *in situ*.

These studies suggest a role for calcium-induced calcium release channels in excitation-contraction coupling. They do not allow us to conclude that calcium-induced calcium release is the mechanism responsible for gating these channels physiologically. Similar studies have negated a role for SH oxidation in e-c coupling. (Supported by AHA, Texas Affiliate and R01 AR34377).

W-AM-C8 MYOPLASMIC pH AND CALCIUM TRANSIENTS FROM INTACT FROG SKELETAL MUSCLE FIBERS SIMULTANEOUSLY INJECTED WITH PHENOL RED AND FURA-2. P. C. Pape, M. Konishi, S. Hollingworth and S. M. Baylor. Departments of Physiology, University of Pennsylvania, Philadelphia, PA and University of Newcastle, Newcastle-upon-Tyne, England.

Intact single fibers were mounted on an optical bench apparatus, stretched to long sarcomere spacing and micro-injected with both phenol red and fura-2 at one fiber location and phenol red alone at a second location (16-17°C). From phenol red absorbance measurements made at various times and at various distances from the injection sites, changes in myoplasmic pH (Δ pH) initiated by action potential stimulation were estimated over a wide range of fura-2 concentrations (0-1 mM). Fura-2 related fluorescence measurements were corrected kinetically to estimate changes in myoplasmic free calcium (Δ [Ca²⁺]), which in turn were used to drive the model of Baylor, Chandler and Marshall (1983) to estimate changes in total myoplasmic calcium (Δ [Ca_T]) released from the sarcoplasmic reticulum (SR). As shown previously (Baylor and Hollingworth, 1988), because of fura-2's calcium-buffering action in myoplasm, larger concentrations of fura-2 result in smaller Δ [Ca²⁺] but larger Δ [Ca_T] responses. In all 7 fibers examined in this study, the amplitude of the Δ pH signal was found to increase as Δ [Ca_T] increased (and Δ [Ca²⁺] decreased). Best fit lines to the Δ pH vs. Δ [Ca_T] data had an average slope of 0.0075 Δ pH units per mM of Δ [Ca_T] and an average intercept of -0.0001 pH units. Through time to peak the time course of Δ pH slightly lagged that of Δ [Ca_T] (time to half-rise lagged by 1-2 ms). Moreover, the negative correlation of Δ pH with Δ [Ca²⁺] argues that the Δ pH response is not artifactually driven by the rise in myoplasmic calcium. These results support the interpretation that the Δ pH measured with phenol red reflects the movement of protons from the myoplasm into the SR as a result of the release of Ca²⁺ ions into the myoplasm.

W-AM-C9 MYOPLASMIC ABSORBANCE SIGNALS FROM ARSENAZO I, A pH/Mg²⁺ INDICATOR DYE. M. Konishi, P. C. Pape, S. Hollingworth and S. M. Baylor. Departments of Physiology, University of Pennsylvania, Philadelphia, PA and University of Newcastle, Newcastle-upon-Tyne, England.

Arsenazo I was pressure-injected into the myoplasm of intact single twitch fibers from frog muscle which had been stretched to long sarcomere spacing. Dye-related absorbance signals were measured, from fibers both at rest and stimulated electrically to give a single action potential. The apparent diffusion constant of the dye in myoplasm, estimated from the resting absorbance of the dye at 520 nm, was found to be $0.47 \pm 0.06 \times 10^{-6}$ cm²/s (mean \pm SEM; 16-17°C). This value is about 1/2 that expected in myoplasm for a freely-diffusible molecule of this size (MW 545), thus indicating that about 1/2 of the dye was bound to relatively immobile myoplasmic constituents.

The arsenazo I resting absorbance spectrum $A(\lambda)$ ($450 < \lambda < 620$ nm) was well-fitted by *in vitro* calibration curves at several combinations of pH and free Mg²⁺. Under the assumption that myoplasmic pH was 6.9, the average value (\pm SEM) of free Mg²⁺ reported by the dye was 4.4 ± 0.5 mM, whereas if pH was 7.1 the corresponding estimate was 2.2 ± 0.2 mM. One component of the dye-related absorbance change ΔA detected during fiber activity was isotropic and likely reflects a small myoplasmic alkalization, since: (1) its spectral dependence was similar to *in vitro* calibrations for a change in pH (and/or a change in Mg²⁺), and (2) the signal amplitude (0.0035 ± 0.0009 ; mean \pm SEM), time to half-rise (9 ms) and time to peak (15 ms) were very similar to that reported previously from the pH indicator dye phenol red (Baylor, Hollingworth and Pape, 1987; see also Pape *et al.*, this meeting). The second component of the arsenazo I ΔA was dichroic, with properties similar to that previously reported for the arsenazo III dichroic signal (Baylor, Chandler and Marshall, 1982), and likely reflects activity of bound and oriented dye molecules.

W-AM-C10 DOES Na⁺/Ca²⁺ EXCHANGE GENERATE A CURRENT IN VASCULAR SMOOTH MUSCLE CELLS FROM RABBIT PORTAL VEIN? Normand Leblanc, and Joseph R. Hume, Dept. of Physiology, Univ. of Nevada School of Medicine, Reno, Nevada, USA, 89557.

The importance of Na⁺/Ca²⁺ exchange for Ca homeostasis in smooth muscle is controversial. We have attempted to identify a macroscopic current that could reflect the electrogenicity of this system in whole-cell voltage clamped smooth muscle cells isolated from rabbit portal vein. The composition of the bath and pipette solutions was designed to inhibit most of the ionic channels, the Na⁺/K⁺ pump, and a possible contribution from SR. With 30 mM NaCl inside and 5 mM Ca outside, various test pulses from -40 to +50 mV from a holding potential of -50 mV elicited a relatively steady outward current. Upon return to the holding potential, a slow inward tail current could be recorded resembling inward creep currents previously identified as Na⁺/Ca²⁺ exchange currents in cardiac cells (Hume and Uehara, *J. Gen Physiol.* 87: 857, 1986; Barceñas-Ruiz et al., *Science* 238: 1720-1722, 1987). External Na replacement by N-Methyl-D-Glucamine enhanced the outward current and reduced the inward tail and the cell contracted promptly. After exposure to a nominally Ca-free solution, readdition of Ca in the medium induces a net outward current (subtracted) that rectifies slightly in the outward direction. Both the outward current and the inward tail current are inhibited by 3,4'-dichlorobenzamil (10 μM). In conclusion, we have identified a component of membrane current that shares some of the properties of Na⁺/Ca²⁺ activity as demonstrated in other excitable cells. However, more experiments are needed to confirm that these currents are indeed generated by the Na⁺/Ca²⁺ exchange system. This work was supported by HL 30143. N. Leblanc is a fellow of MRC of Canada and J.R. Hume is an established investigator of AHA.

W-AM-D1 β -TURN STABILITY IS DETERMINED BY GLYCOPEPTIDE INTRAMOLECULAR H-BONDS. G.D. Fasman, M. Hollósi*, and A. Perzcel*, Dept. of Biochemistry, Brandeis University, Waltham, MA 02254-9110, and *Institute of Organic Chemistry, L. Eötvös University, Budapest, Hungary.

Anomeric mixtures of 2,3,4,6-tetra-O-acetyl-D-gluco-, -D-galacto-, and -D-mannopyranosides of Boc-X-Y-NHCH₃ dipeptides (X-Y=Pro-Ser, Pro-D-Ser, Val-Ser, Val-D-Ser and Gly-Ser) have been synthesized. Circular dichroism and infrared spectroscopic studies were performed to characterize the peptide backbone conformation and examine the possible formation of intrapeptide and glyco-peptide intramolecular H-bonds. It was found that O-glycosylated peptides containing a D-serine residue are likely to adopt a type II β -turn while those with the Pro-Ser or Val-Ser sequence feature a type I(III) β -turn in solution. Glycosylation also increases the magnitude of the CD bands, characteristic of the given type of β -turns, which can be interpreted as an indication of the stabilization of the folded backbone conformation. IR data showed that in non-polar solutions, the peracetyl glycopeptides adopt both single- and double H-bonded conformations whose ratio, in some cases, depends on the position at C-2' of the H-bond acceptor acetoxy group. These data suggest that five-, seven-, or ten-membered glyco- β -turns, may play an important role in fixing the steric orientation of the carbohydrate antennae systems in glycoproteins. Supported by NSF Grant # DMB-8512570.

W-AM-D2 SPECTROSCOPIC AND DSC STUDIES PROVIDE EVIDENCE FOR STABLE INTERMEDIATES IN THE THERMAL UNFOLDING AND REFOLDING PATHWAY OF SERUM RETINOL BINDING PROTEIN. D. Vincent Waterhouse[#], Christie G. Brouillette,⁶ Fred Fish[#] and Donald D. Muccio[#]. Departments of Chemistry[#] and Medicine⁶. University of Alabama at Birmingham, 35294

Circular dichroism (CD) and differential scanning calorimetry (DSC) were used to study the thermal unfolding and refolding of human serum retinol binding protein (sRBP) over the 25 to 85 °C temperature range. The spectroscopic thermal unfolding changes were reversible up to 70 °C; above this temperature reversibility occurred only when there was a sufficient amount of all-trans-retinol present (two equivalents or more) during the refolding. The analysis of thermal changes in the far-UV CD spectra was consistent with a two-state process. The transition was centered at 78 °C and a van't Hoff enthalpy of 120 kcal/mol was determined. In contrast to this result, the analysis of the thermal changes in the near-UV CD spectra was shown to fit well to a three-state process, with transition temperatures centered at 63 and 75 °C and respective enthalpies changes of 30 and 110 kcal/mol. The DSC curve, which was centered near 78 °C, was asymmetrical. The van't Hoff enthalpy was found to be less than the calorimetric enthalpy which indicated that intermediates were present in the thermal unfolding pathway. A sequential fit to the DSC curve required that two high enthalpy transitions be positioned close together at 74 and 78 °C. A low enthalpy transition could be placed at 63 °C, which was revealed from the near-UV CD analysis, without degrading the quality of the fit. Together, the spectroscopic and DSC results were found to be most consistent with a three-stage (four-state) linear model in which the native protein (N) thermally unfolds to U via two intermediates, I/R and I (N \rightleftharpoons I/R \rightleftharpoons I + R \rightleftharpoons U + R). The expected conformations of I/R, I and U are discussed, and the biological implications of the unfolding mechanism are considered.

W-AM-D3 PRELIMINARY CRYSTAL STRUCTURE OF ISOCITRATE DEHYDROGENASE FROM *ESCHERICHIA COLI*. J. Hurley¹, V. Ramalingam¹, N. Helmers¹, P. Thorsness², D.E. Koshland, Jr.² and R. M. Stroud¹, ¹Dept. of Biochemistry and Biophysics, University of California, San Francisco and ²Dept. of Biochemistry, University of California, Berkeley.

The Krebs cycle enzyme isocitrate dehydrogenase isolated from *E. coli* is regulated by a reversible phosphorylation-dephosphorylation cycle. Inactivation of IDH by phosphorylation is essentially complete, and allows the cell to shift acetyl groups from energy metabolism to biosynthesis during growth on acetate. IDH is an NADP-linked dehydrogenase of 416 residues, and exists as a dimer. Serine 113 is the site of phosphorylation, and oligonucleotide-directed mutagenesis experiments have shown that the negative charge on the phosphoserine mediates inactivation. The conversion between phosphorylated and dephosphorylated forms is catalyzed by a single bifunctional enzyme, IDH kinase/phosphatase. The kinase/phosphatase is saturated by physiological concentrations of IDH, which leads to enhanced sensitivity to environmental changes by the mechanism of zero-order ultrasensitivity. Protein phosphorylation is an important regulatory mechanism in many areas of cell and molecular biology, and the three-dimensional structures of the phosphorylated and dephosphorylated forms of IDH are of interest primarily for this reason. Crystals of both forms, as well as crystals of the S113D mutant, have been grown. An interpretable map has been calculated at 2.8 angstroms nominal resolution for the dephosphorylated enzyme by combining single isomorphous replacement and density modification techniques. Most of the main chain has been traced, revealing a two-domain, α/β structure.

W-AM-D4 THE STABILISATION OF HALOPHILIC MALATE DEHYDROGENASE. G. Zaccai and F. Cendrin, Institut Laue Langevin, 156X, 38042 Grenoble Cedex, FRANCE, and Y. Haik, N. Borochoy and H. Eisenberg, Polymer Research Department, The Weizmann Institute of Science, Rehovot, ISRAEL.

Malate dehydrogenase from *Halobacterium marismortui* is only stable in high concentration of salt. Its structure and stability cannot be explained in terms of the usual effects of salts on protein structure. For example, the structure of this enzyme can be stabilised by high concentrations of Mg^{++} or Li^+ , "salting-in" ions which favour protein unfolding. Results of enzymatic activity and stability measurements in different salt solutions (K-phosphate, a strong "salting-out" agent - NaCl and KCl, which are mildly "salting-out" and $MgCl_2$) combined with data from neutron scattering, ultracentrifugation and quasi-elastic light scattering experiments led to a novel model for the structural stabilisation of the halophilic protein. The model has a hydrophobic core and loops rich in charged amino-acid residues protruding into the solvent. At high concentrations of KCl, NaCl or $MgCl_2$, a solution particle is formed in which the loops of the protein dimer interact with a large number of salt and water molecules. The halophilic protein is stabilised by specific protein-salt-hydrate bonds formed by the loops, which would have to be stronger than salt hydrate bonds in the bulk solvent. The thermodynamic stability of the solution particle, is mainly enthalpy driven, unlike non-halophilic globular proteins in which entropy terms are dominant for stabilisation close to room temperature. Halophilic malate dehydrogenase, however, can also be stabilised by more classical mechanisms. The protein was found to be active and stable in 1.5 M K-phosphate, with hydration interactions and thermodynamics of stabilisation similar to those of non-halophilic globular proteins.

W-AM-D5

X-ray Absorption Study of MbCO Photo-products at 70K

K. Zhang, B. Chance and K. S. Reddy,
Biochem/Biophys, Univ. of Penn; & ISFS, Univ. City Sci. Ctr, Phila, PA 19104

The structure determination of MbCO photo-products could elucidate the mechanism of ligand rebinding process and protein dynamics. We have used X-ray absorption spectroscopy to study myoglobin photo-products at 60 - 80K temperature region with on line optical pumping and monitoring. The heme environment, especially for the location of the CO bond, require highly precise, time consuming EXAFS data. An error analysis for determining the iron environment in the MbCO photo-product indicated that the single CO bond distance determined by least-squares fitting could be substantially in error due to more than one local minima derived from the least-squares fitting. A simulation performed on the near edge region shows that the signal is sensitive to a single ligand such as CO bond in MbCO and is able to give the Fe-CO distance in the protein more accurately.¹ The structure of the 70K photo-product determined is confirmed to be different from the structure of the photo-products at lower temperatures. Supported by NIH grants HL 18708 and RR 01633.

(1). K. Zhang, B. Chance and K. S. Reddy, *Proceedings of XAFS V*, Seattle, 1988, to be published.

W-AM-D6 MAPPING OF THE INTERMOLECULAR CONTACTS WITHIN SICKLE HEMOGLOBIN FIBERS

L. J. Gross, S.J. Watowich and R. Josephs. Laboratory for Electron Microscopy and Image Analysis.
Department of Molecular Genetics and Cell Biology, University of Chicago, Chicago, IL 60637.

Sickle-cell anemia is caused by the polymerization of deoxyhemoglobin S (HbS) molecules to form helical fibers. Since these fibers are responsible for erythrocyte sickling, the determination of HbS fiber structure and intermolecular contacts is important for the design of anti-sickling agents. Furthermore, knowledge of the intermolecular contacts provides insights into the factors which drive the assembly and stabilization of macro-molecular structures.

Electron microscopy has demonstrated that the fiber consists of 7 double strands of HbS molecules twisted around the fiber axis. These studies have determined the fiber pitch, the molecular coordinates, the pairings of molecules forming double strands, and the orientations of the 7 double strands. We have combined X-ray crystallographic coordinates of the HbS double strands with the low resolution electron microscopy data to calculate the intermolecular contact regions within the fiber.

The known effects of additional point mutations on the formation of HbS fibers can be understood in light of the calculated intermolecular contacts. Of the 26 known mutations that affect fiber formation, 7 are located in contact regions between double strands, 15 are located in contact regions within double strands, and 4 are near the axial contact regions within strands. Of 27 known mutations which do not influence fiber formation, only 3 are located within contact areas; these mutations appear not to alter the chemical or steric properties of those regions. Furthermore, the number of axial contacts within double strands diminishes with increased distance from the fiber axis; a hypothetical eighth strand added to the exterior of the fiber would have no axial contacts.

The calculated atomic structure of the fiber is being refined by energy minimization and molecular dynamics procedures and will be used to improve existing models of fibers and to investigate molecular interactions between aligned fibers. This work is supported by NIH grants HL07722 (SJW) and HL22654 (RJ).

W-AM-D7 THE Ca(II) BINDING SITE OF A BACTERIAL SENSORY RECEPTOR: METAL BINDING SPECIFICITY AND KINETICS. Brian W. Buoscio and Joseph J. Falke, Department of Chemistry and Biochemistry, University of Colorado, Boulder CO 80309-0215.

Although Ca(II) binding sites play central roles in biological signaling pathways, the specificity and kinetics of metal binding to these sites is not well studied. Using fluorescence techniques and submicromolar concentrations of binding sites, we have systematically studied metal binding to the *E. coli* soluble sensory receptor for galactose and glucose (galactose binding protein, GBP). The known structure of GBP contains a Ca(II) site similar to the EF-hand sites of eukaryotes (1.9 Å resolution, F. Quiocho et al). When the site is occupied by Tb(III), excitation of nearby tryptophan chromophores results in efficient energy transfer and subsequent Tb(III) fluorescence. Metals which compete with Tb(III) for binding decrease the Tb(III) fluorescence, enabling analysis of site specificity. Our results show that Group Ia metals do not bind to the site (Li(I), Na(I), K(I), and Rb(I) were tested). In Group IIa only Ca(II) and Sr(II) bind (Mg(II), Ca(II), Sr(II) and Ba(II) were tested). All lanthanides tested bind (La(III), Eu(III), Gd(III), Tb(III), Dy(III), Ho(III) and Er(III)). The data place quantitative limits on the dissociation constant for the binding of each metal. Of the metals encountered by the protein in its biological environment, only Ca(II) binds; in this sense the site is highly specific. It is not yet clear which structural features of the site determine specificity: the described assay will enable future analysis of the relationship between structure and specificity in this and other Ca(II) binding proteins. Other results to be discussed will include the kinetics of metal binding to the Ca(II) site, and the implications of these kinetics for the biological role of Ca(II) in the *E. coli* sensory system. (Supported by NIH grant GM40731-01).

W-AM-D8 REDUCED BPTI HAS A COMPACT STRUCTURE

Elisha Haas and Dan Amir, Department of Life Science, Bar-Ilan University Ramat-Gan, and Departments of Chemical Physics and Biophysics Weizmann Institute of Science, Rehovot, ISRAEL.

The conformation of reduced bovine pancreatic trypsin inhibitor, R-BPTI, under reducing conditions, was monitored by measurements of non-radiative excitation energy transfer efficiencies, E , between a donor probe attached to N-terminal arg⁺ residue and an acceptor attached to one of the lysine residues (15, 26, 41 or 46) (D. Amir and E. Haas, (1987), *Biochemistry*, 26, 2162-2175). High excitation energy transfer efficiencies which approach those found in the native state were obtained for the reduced labeled BPTI derivatives in 0.5M guanidinium hydrochloride, (GuHCl) and 4 mM DTT. Unlike the dependence expected for a random coil chain, E does not decrease as a function of the number of residues between the labeled sites. The efficiency of energy transfer between probes attached to residues 1 and 15, in the reduced state is higher than that found for the same pair of sites in the native state or reduced unfolded, (in 6M GuHCl), state. This segment also shows high dynamic flexibility. These results indicate that the overall structure of reduced BPTI under folding (but still reducing) conditions shows high population of conformers with interprobe distances similar to those of the native state. Reduced BPTI seems to be in a molten globule state characterized by a flexible, compact structure, which probably reorganizes into the native structure when the folding is allowed to proceed under oxidizing conditions.

W-AM-D9 IMAGE ANALYSIS REVEALS PERIODIC STRUCTURE IN NEGATIVELY STAINED SPECTRIN.

A. M. McGough, B. Carragher, and R. Josephs. Laboratory for Electron Microscopy and Image Analysis, Department of Molecular Genetics and Cell Biology, University of Chicago, Chicago, IL, 60637.

The erythrocyte membrane is stabilized by a two-dimensional cytoskeleton located on its cytoplasmic face. This skeleton consists of long molecules of spectrin which link short dodecamers of actin into a network. A vital property of the red blood cell membrane, elastic response to transient deformation, is commonly attributed to spectrin. Erythrocyte spectrin consists of two distinct polypeptide chains, termed *alpha* (240 KD) and *beta* (220 KD), which laterally associate to form a flexible heterodimer approximately 1000 Å long when fully extended. Dimers associate head to head to form tetramers, the dominant form of spectrin in the cell. The conformation assumed by spectrin tetramers in the cell is not known, however calculations based on the number of molecules per unit area indicate that it is not fully extended in its native state. We have applied correlation averaging techniques to electron micrographs of negatively stained membrane skeletons in order to better relate spectrin's structure to its functional properties.

Examination of skeletons revealed thin spectrin molecules approaching 2000 Å in length and thicker spectrin molecules approximately 1500 Å in length. Fourier analysis of the thick spectrin particles revealed periodic features. In both Fourier filtered and correlation averaged images two thin strands appeared to twist around one another, overlapping at intervals of about 55 Å. We believe the twisting strands visible in micrographs of spectrin represent individual *alpha* and *beta* subunits. We hypothesize that the thick spectrin tetramers seen in isolated membrane skeletons have shortened by the regular coiling of their *alpha* and *beta* strands. This coiling may represent a means of adjusting spectrin's length under various physiological conditions. In particular, spectrin may assume a similar coiled structure in the cell where the tetramer is also not fully extended. Supported by NIH grant HL22654 (RJ).

W-AM-D10 X-RAY AND NEUTRON DIFFRACTION STUDIES OF FILAMENTOUS BACTERIOPHAGE PF1 Raman Nambudripad, Wilhelm Stark, and Lee Makowski, Department of Physics, Boston University, Boston, MA 02215

The 65 Å diameter, 2 micron long Pfl particle is made up largely of 7200 identical protein subunits coating its single-stranded circular DNA genome. X-ray fiber diffraction patterns of magnetically oriented particles contain data extending to at least 3.5 Å resolution. Heavy atom binding causes alterations in the helical symmetry of the particles precluding the use of isomorphous derivatives for phasing of the pattern. Neutron diffraction of specifically deuterated phage particles has been used to determine the location of 19 of the 46 amino acid residues in the coat protein. The relative positions of these 19 amino acids define the conformation and fold of most of the coat protein. Most of the coat protein appears to be contained in a pair of alpha helices connected by a short loop of non-helical peptide. The locations of the 19 residues are being used as a starting point for the construction of molecular models being refined against the 3.5 Å resolution X-ray data. This refinement should result in a detailed description of the structure of the protein coat to 3.5 Å resolution. The interactions among coat proteins are responsible for maintaining the structural viability of the virus particles over a broad range of conditions. These same interactions provide for the mechanical flexibility of the particles, and the observed transitions in helical symmetry. Analysis of intermolecular interactions has provided insight into the means by which the proteins can maintain interactions within a flexible structure.

W-AM-D11 THE STRUCTURE OF FILAMENTOUS BACTERIOPHAGE M13

Marc J. Glucksman, Sarama Bhattacharjee, Leon Specthrie and Lee Makowski
Dept. of Physics, Boston University, Boston, MA 02215
Dept. of Biochemistry and Molecular Biophysics, Columbia, New York, N.Y. 10032

Filamentous bacteriophage M13 is a flexible particle about 65 Å in diameter and about 9000 Å in length. A single-stranded loop of DNA extends along its helical axis and is coated by 2700 copies of the Gene 8 protein. Several minor proteins are located at each end of the particle. X-ray fiber diffraction patterns of magnetically oriented particles extend to at least 2.4 Å resolution. A combination of model building and isomorphous replacement has been used to determine the phage structure to 7 Å resolution. The positions of the amino terminus, tyr 21 and tyr 24 have been defined by the locations of the heavy atom labels. The relative positions of these three residues are consistent with a largely alpha helical conformation for the coat protein. Because of the flexibility of the tyrosine side chains and the modified amino terminus, there is some uncertainty in the locations of the alpha carbons of these residues. Consequently, we cannot, as of yet, rule out the possibility of some non-alpha helical conformation in the coat protein. The volume available to DNA along the axis of the virus particle appears to be non-uniform suggesting a complex conformation for the viral DNA.

W-AM-D12 CRYOELECTRON MICROSCOPY AND IMAGE AVERAGING OF BACTERIAL FLAGELLAR BASAL BODY.

N.R.Francis, G.E.Sosinsky, M.J.B.Stallmeyer, and D.J.DeRosier, Rosenstiel Basic Medical Sciences Research Center, Brandeis University, Waltham MA 02254-9110.

The *Salmonella typhimurium* basal body, a component of the flagellar rotary motor, is composed of four rings (M,S,L,P) threaded on a coaxial rod. Averages of negatively stained preparations of basal bodies revealed an extra ring between the L and P rings. The averaged images obtained from frozen-hydrated preparations show four lobes of density rather than a continuous ring. This feature between the L and P rings appears to be a cylindrical wall which joins the two rings. In the frozen-hydrated preparation, the hollow, axial rod on which the rings sit, when superposed on the wall gives the appearance of four lobes of density. The solid ring seen in negatively stained preparations arises from lack of stain penetration into the inside of the LP-rod complex. The S,L, and P rings appear to be cylindrically symmetric, although cryoelectron micrographs reveal differences in the M ring appearance which may be interpreted as non-cylindrical symmetry; that is, as being divided into subunits. The degree to which the structure appears cylindrically symmetric can be judged from analysis of the variance maps produced as part of the averaging process. To further analyze the subunit organization of the basal body, we incubated preparations at low pH. Under this condition, the basal bodies dissociate into subassemblies (Sosinsky et al.1988, Biophys. J. 53, 417a). One subassembly consists of a basal body lacking the M and S rings but having the rod on which they sit. Another lacks this portion of the rod. This suggests the rod is composed of two parts: one extending from the P ring into the M-S ring complex and the other from the hook through the L and P ring complex.

W-AM-E1 Footprinting Analysis of A Group of Minor Groove Binding Lexitropsin Ligands. Koren Kissinger¹, Moses Lee², J. William Lown², and James C. Dabrowiak¹ (Intro. by P. Dunham). ¹Department of Chemistry, Syracuse University, Syracuse, New York 13244-1200, ²Department of Chemistry, University of Alberta, Edmonton, Alberta, Canada T6G 2G2.

A series of lexitropsin ligands, structurally related to netropsin have been prepared and studied using DNase I footprinting methods. The optically active natural products dihydrokikumycin and anthelvincin bind to AT rich sites on a 139 bp fragment from pBR-322 DNA. Comparative studies with the compounds indicate that ligand size and the location of the stereocenter affects the binding affinity of the compound. For lexitropsin ligands possessing two netropsin type "feet" linked via a tether, the structure of the tether influences the size of the binding site and the affinity of the ligand toward its interaction sequences. Parallel studies with a bis N-methyl imidazole ligand involving two different restriction fragments indicated that this ligand prefers to bind to sequences rich in GC content of the type, (GC)₂(AT)(GC). Quantitative MPE footprinting investigations involving this ligand revealed that the system can be analyzed using a DNase I type redistribution model. Since this probe was able to cleave DNA within a binding site while the site was occupied by ligand, determining the dimensions of the site from the experimentally-derived footprinting plots proved to be difficult.

W-AM-E2 ANALYSIS OF BINDING MODE AND SPECIFICITY IN DNA INTERACTIONS: COOPERATIVITY AND INDUCED FIT INTERACTIONS IN INTERCALATION AND GROOVE-BINDING COMPLEXES. W. David Wilson, Farial A. Tanious, Henryk J. Barton, Robert L. Jones⁺, M.K. Venkatramanan, David W. Boykin, Donald B. Harden, Lucjan Strekowski, Departments of Chemistry, Georgia State University and ⁺Emory University, Atlanta, Georgia

Of interest in both theoretical studies and molecular design are the energetic and structural differences between intercalation and groove-binding interactions, and the conformational changes induced in DNA by both types of binding mode. We have investigated the structural requirements for intercalation and groove binding in polyaromatic systems. Results with bicyclic and tricyclic unfused aromatic molecules with terminal basic functions indicate that the distinction between intercalation and groove binding may be quite subtle. Molecules with highly twisted aromatic systems do not intercalate or fit well into the minor groove, and they generally bind poorly to DNA. On the other hand some tricyclic molecules that are essentially planar bind quite well in the minor groove while significantly twisted tricyclic compounds can intercalate. The groove-binding molecules display cooperative binding isotherms and high specificity for A-T base-pairs. Some twisted intercalators display a slight A-T selectivity which might be due to the higher intrinsic propeller twist of A-T relative to G-C base-pairs. Binding of the propeller-twisted intercalators probably involves an induced-fit type of binding mechanism and under some conditions they can switch to an external binding mode. A number of factors have been identified which are critical in selecting the DNA binding mode for the unfused aromatic systems and it now appears that intercalation and groove-binding modes should be viewed as two potential wells on a continuous energy surface.

W-AM-E3 UNWINDING OF SUPERCOILED DNA INDUCED BY NONCOVALENT AND COVALENT BINDING OF POLYCYCLIC AROMATIC HYDROCARBON METABOLITES. N.E. Geacintov, S.E. Carberry, C.E. Swenberg* and R.G. Harvey**; Department of Chemistry, New York University, New York, NY 10003; *Armed Forces Radiobiology Research Institute, Bethesda, MD 20814; **Ben May Laboratory for Cancer Research, The University of Chicago, Chicago, IL 60637.

We have investigated the interactions of the two enantiomers of *trans*-7,8-dihydroxy-*anti*-9,10-epoxy-benzo[a]pyrene (BPDE), the most mutagenic metabolites of benzo[a]pyrene, with supercoiled ϕ X174 DNA (RF I). In mammalian cell systems, the enantiomer (+)BPDE is more mutagenic than the (-) stereoisomer, and is also a strong tumorigen, while the (-) isomer is not. The differences in the modes of interactions of these two stereoisomers with nucleic acids, and the types of DNA damage produced, are therefore of great interest. Since BPDE is unstable in aqueous media, the kinetic flow dichroism technique developed earlier (Yoshida et al., *Biochemistry*, 1987, 26, 1351) was utilized to follow the effects of noncovalent complex formation on the superhelicity of ϕ X174. In spite of the fact that both BPDE enantiomers form intercalation complexes with ϕ X174 with the same affinities, the degree of unwinding induced by the (+) enantiomer is about 3 times higher than in the case of the (-) isomer. Agarose gel migration patterns are strongly affected by the covalent binding of the (+) enantiomer to DNA (about $r=0.01$, BPDE residues/base); however, in the case of the (-) enantiomer, unwinding is observed only at values of $r > 0.01$. These findings are related to the structural properties of the covalent BPDE-DNA adducts determined by other physical techniques.

W-AM-E4 THE APPLICATION OF FLUOROPHORE LABELED DNA TO THE STUDY OF HYBRIDIZATION KINETICS AND THERMODYNAMICS. Larry E. Morrison and Lucy M. Stols, Amoco Technology Company, P.O. Box 400, Naperville, IL 60566.

DNA hybridization measurements in solution are generally performed using either absorbance spectroscopy or calorimetry, both of which require relatively high concentrations of DNA. In order to utilize a more sensitive technique, such as fluorescence, a fluorescent label is required which responds to the state of hybridization. We have found that the emission of fluorescein attached to the 5'-terminus of a DNA strand is quenched upon hybridization to a complementary strand of DNA containing any of several fluorophores attached to the 3'-terminus. The quenching fluorophores include pyrenebutanoate, sulforhodamine 101, and eosin. Quenching as great as 93% was observed in the presence of excess quencher strand. The fluorescence response to hybridization allowed DNA melting curves to be recorded at 50 μ M strand concentrations. In addition, the rate of DNA association was measured using strand concentrations as low as 10 μ M. Using fluorescence measurements, the association and dissociation rate constants for 10 a base long pair of complementary oligomers were determined as a function of temperature. The hybridization rate constant of the 10-mer was found to increase from $2.2 \times 10^6 \text{ s}^{-1} \text{M}^{-1}$ at 3°C to $1.0 \times 10^7 \text{ s}^{-1} \text{M}^{-1}$ at 35°C with an activation energy of 7.5 kcal/mol. The dissociation rate constant increased from $1.9 \times 10^{-3} \text{ s}^{-1}$ at 24°C to 0.12 s^{-1} at 40°C with an activation energy of 53 kcal/mol. Rate constants for other oligomers were measured and the enthalpy and entropy changes accompanying hybridization were determined from melting temperatures recorded at various strand concentrations.

W-AM-E5 FLUOROMETRIC ANALYSIS OF THE LONG-WAVELENGTH ABSORPTION BAND OF N-7 METHYLATED GMP INTO THE CONSTITUENT BANDS OF THE TWO ELECTRONIC STATES. Solon Georghiou, Shen Zhu and Thomas D. Bradrick, Biophysics Lab., Dept. of Physics, Univ. of Tennessee, Knoxville, TN 37996.

Steady-state measurements of fluorescence anisotropy and quantum yield were used to resolve the long-wavelength absorption spectrum of 7-methyl GMP in glycerol at room temperature into component spectra that correspond to the electronic transitions I and II present in that spectral region. Of the four different models tested, the only one that adequately describes the data involves emission exclusively from state I, with state II converting to it with an efficiency of about 60%. At 260 nm state II absorbs about 17% more than state I. An isosbestic point exists at about 272 nm. The oscillator strengths of the electronic transitions I and II are 0.17 and 0.16, respectively. Both spectra, and especially that associated with state I, exhibit vibronic structure and overlap with each other to a great extent. This is in contrast to the absorption spectra of all the other nucleotides which are known to lack structure. The fluorescence spectrum is structureless, however, and this disparity indicates that the ground and excited states have different nuclear configurations. This analysis should be approximately valid for the nonmethylated nucleotide as well in view of the reported finding that the directions of the transition dipole moments of guanine are not very sensitive to chemical substitutions. The relevance of these findings with respect to the occurrence of energy transfer by vibronic resonance between neighboring guanines in nucleic acids will be briefly discussed. (Supported by NIH grant GM38236.)

W-AM-E6 EFFECT OF CRYPTANDS ON THE HELIX-COIL TRANSITION OF DNA: ION RADIUS EFFECTS

David A. Knoll¹, Victor A. Bloomfield¹, Masakatsu Ueno², Beth Trend² and D. Fennell Evans², Departments of Biochemistry¹ and Chemical Engineering and Materials Science², University of Minnesota, St. Paul MN 55108.

Cryptands are macrocyclic polyethers which are able to encapsulate various metal cations with high affinity. The resulting cryptate complex has the same charge as the metal ion, but a radius several Å larger. We have used the cryptand C222 [Evans et al. (1988) J. Phys. Chem. 92:784], which strongly binds K^+ , to study the effect of ion size on DNA melting. With calf thymus DNA and K^+ as the sole cation, T_m varies linearly with the log of ionic strength, over the range 2.5 to 60 mM. With all the K^+ sequestered by a slight molar excess of C222, the slope is approximately the same but T_m is decreased by about 13°C. Thus, our results indicate that when the ionic radius of K^+ is increased by complexation with C222, the larger cation stabilizes the double helix less effectively. This is in accord with considerations based on Hill's [(1955) Arch. Biochem. Biophys. 57:299] theory for the dependence of the electrostatic free energy W_{el} of a long cylindrical ion on its radius of exclusion. Experiments with other cations are in progress.

W-AM-E7 SCANNING TUNNELING MICROSCOPY (STM) OF NUCLEIC ACIDS

Gil Lee, Patricia Arscott*, Victor A. Bloomfield*, and D. Fennell Evans, University of Minnesota, Dept. of Chemical Engineering, Minneapolis, and Dept. of Biochemistry*, St. Paul.

STM of biological material is inherently difficult: topographical features are often highly irregular and easily perturbed, and conductivity can vary from one part of a molecule to another. STM studies of DNA^{1,2} have thus far not achieved the resolution and detail of conventional electron microscopy. By varying methods of sample preparation we have gotten high resolution images of DNA on highly oriented pyrolytic graphite after freeze-drying, or drying at ambient temperatures. In some experiments, spermidine³⁺ or cobalt hexamine (III) was added to the DNA to neutralize its negative charge and thereby increase the probability of side-by-side aggregation and alignment. The images clearly show the helical twist of DNA fibers, and measurements of their diameter and periodicity are consistent with dimensions of A- and B-form DNA obtained by other means. This work is currently being extended to RNA and synthetic polynucleotides of known conformation.

¹Travaglini, G., Rohrer, H., Amrein, M. and Gross, H. (1987) *Surface Sci.* 181: 380-390

²Bennig, G. (1986) *Bull. Am. Phys. Soc.* 31: 217

W-AM-E8 PROBING THE HYDRATION OF THE MINOR GROOVE OF A·T SYNTHETIC DNA POLYMERS. Luis A. Marky¹ and Donald W. Kupke², ¹Department of Chemistry, New York University, New York, NY 10003; ²Department of Biochemistry, School of Medicine, University of Virginia, Charlottesville, Va 22908.

The structure of poly dA·poly dT has been the subject of intensive investigation by a wide variety of experimental techniques. These studies have led investigators to propose that this homopolymer adopts a heteronomous structure in which the poly dA strand is in the A-helix conformation, and the poly dT strand in the B-helix conformation. It was also noted that the homopolymer duplex does not undergo a conformational transition to the A form as the water activity is decreased. In addition, unusual effects have been found in the interactions of ligands with the homopolymer, where as the interactions with the alternating polymer, poly dAT duplexes, are similar to that of any other DNA polymer.

We have used netropsin (a minor groove ligand specific to A·T base pairs) as a probe of the hydration of the minor groove of these two polymers. The polymers were dissolved in a 10 mM sodium phosphate buffer at pH 7.0, sonicated, and dialysed exhaustively against the same buffer, and were of similar viscosities. The volume change, ΔV , that accompanies binding of netropsin to these polymers was measured with a densimetric method. With the homopolymer we obtained a putative water release equal to 97 ml per mole of bound ligand, and with the alternating polymer a water uptake of 16 ml per mole of bound ligand. Here the striking differential effect suggests that the homopolymer duplex compresses more water (or is more extensively hydrated by about 6-7 molecules of water per binding site). These results correlated conveniently with the known ΔH and ΔS binding parameters obtained with the same system. (Funded in part by NIH GM-34938)

W-AM-E9 THE ROLE OF HYDRATION IN THE FORMATION OF 28 BASE PAIRS.

A.A. Rashin, Dept. Physiology and Biophysics, Mount Sinai School of Medicine, New York, NY 10029; P. Hobza, Inst. of Organic Chemistry and Biochemistry, Czechoslovak Academy of Sciences, Prague 6, Czechoslovakia.

The role of hydration in the formation of 28 Watson-Crick and Hoogsteen base pairs is studied with the recently developed method based on the continuum electrostatics, and an ab initio SCF method, corrected for the basis set superposition error and London-type expression for the dispersion energy. The zero point energy and rotational-translational-vibrational contributions to the entropy of the base pair formation are also evaluated. It is found that the GC Watson-Crick pair has the lowest association energy (1 kcal/mole), and the AT pair has the association energy of 2.6 kcal/mole. We have found five more pairs with association energies between these two values, with four of them lower than 2 kcal/mole, and a total of eight pairs with association energies below 3 kcal/mole. As a rule the better two bases interact with each other the better they also interact with water when separated, and thus a better electronic complementarity is often compensated by a larger loss of hydration. These results suggest that the electronic complementarity alone cannot determine the genetic code, and other factors such as the connectivity of the chain, the conformation of the backbone, etc. can be crucial. We also demonstrate that our method for the computation of enthalpy differences based on the continuum description of the solvent leads to the results similar to the results of the molecular free energy perturbation methods in applications where entropy changes are not expected to be very large.

W-AM-E10 STACKING OF INDOLE WITH PURINES AND PYRIMIDINES.

Predrag Ilich,

Department of Biochemistry and Molecular Biology, Mayo Foundation, Rochester, Minnesota 55905.

Theoretical study indicates near UV transitions that discriminate coplanar stacking of indoles with purine and pyrimidine bases from random aggregation. Further analysis suggests possibility of distinction among intercalating geometries on basis of (i) first order interaction between electric dipole transition moments in indole and a base (Figure) and (ii) second order, intermolecular charge transfer electronic transitions. Evaluation of these effects in view of experimental techniques suggests Stark effect perturbed UV absorption as a tool for analysis of certain protein-DNA interactions. Supported in part by grant GM34847.

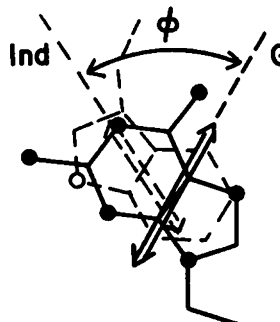


Figure: Directions of transition moments of the lowest observed singlet bands, for a particular stacking geometry of indole (Ind) and guanine.

W-AM-E11 HYPERCYCLIC NETWORKS OF SELF-SPLICING RNAs

Enrico Di Cera Istituto di Fisica, Universita' Cattolica, Largo F. Vito 1, 00168 Roma, Italy.

Template-dependent RNA synthesis by ribozymes has been suggested as a possible mechanism for prebiotic nucleic acid replication [Cech, T.R. (1986) PNAS 83, 4360]. The elementary self-replicative unit is assumed to be constituted by a double-stranded RNA with a ribozyme which specifically catalyzes the synthesis of the parent RNA. Extension of the Cech model to include ribozyme-dependent catalysis of RNAs other than the parent one leads to consideration of hypercyclic networks of self-organization. The dynamical properties of such networks reflect the nature of imperfect catalysts of self-splicing RNAs [Di Cera et al. (1988) PNAS 85, 5923]. The results are discussed in relation to the hypercycle theory [Eigen, M. & Schuster, P. (1979) The Hypercycle, Springer-Verlag].

W-AM-E12 STIMULATION OF BIOSYNTHESIS BY ELECTROMAGNETIC FIELDS. Martin Blank* and Reba Goodman**, Departments of *Physiology and Cellular Biophysics and **Pathology, Columbia University New York, NY 10032.

An electrochemical model has successfully described the opening/closing reactions of voltage gated channels and the ion flows during nerve excitation (Blank, BBA 906:227, 1987). The model also predicts that the charged surfaces involved in biosynthesis should experience frequency dependent switching in alternating electromagnetic fields. We have analyzed published data for both RNA and polypeptide biosynthesis and find that the distributions of molecular weights have the predicted dependence on the frequency of the applied field. The mRNA in cells exposed to 220 Hz sine waves shows a greater augmentation of low molecular weights than cells exposed to 72 Hz sine waves, despite the absolute decrease in mRNA synthesis with increasing frequency. Data on the synthesis of 53 major polypeptides also show an augmented synthesis of lower (20-50 kD) molecular weight polypeptides, and a reduced synthesis in the 50-90 kD molecular weight range (Blank and Goodman, Bioelectrochem. Bioenerg. in press). The new proteins synthesized during electromagnetic or thermal stress have properties that would be expected if they arose from interference with biosynthesis. They tend to have lower molecular weights and are more highly charged. The number of new proteins divided by the amount synthesized increases with the frequency. The electrochemical model also provides a rationale for the effects of endogenous electrical stimulation during nerve excitation on long term potentiation and learning. (We thank the ONR and EPRI for their support.)

W-AM-F1 Ca^{2+} ACTIVATION AND VOLTAGE DEPENDENCE OF THE PARTIAL REACTIONS OF THE Na/Ca EXCHANGE IN SQUID AXONS UNDER SYMMETRICAL IONIC CONDITIONS. R. DiPolo and L. Beaugé, CBB, IVIC, Apdo. 21827, Caracas 1020A, Venezuela. Div. de Biofísica M.y M. Ferreyra 5000 Córdoba, Argentina. The activation of the Na/Ca exchange by Ca^{2+} , Ca^{2+} and the effect of changes in membrane potential on the different modes of operation of the Na/Ca exchange ($\text{Na}^+/\text{Ca}^{2+}$, $\text{Ca}^{2+}/\text{Na}^+$, $\text{Ca}^{2+}/\text{Ca}^{2+}$ and Na^+/Na^+ exchanges) was explored in axons externally perfused and internally dialyzed under similar ionic conditions. Na^+ and Ca^{2+} -dependent Ca efflux components were measured in Na^+ or Li^+ containing medium respectively. Ca^{2+} and Na^+ -dependent Na efflux components were measured in Li^+ or Na^+ containing medium. Axons were voltage-clamped to 0 mV throughout the experiment. The voltage dependence of these components was measured over the range of +20 to -40 mV. The results show: i) under complete symmetrical conditions Ca ions activate with high affinity from inside (22 μM) and low affinity from outside (300 μM). ii) A similar voltage dependence (about 26% change per 25 mV) was obtained for all modes of operation of the Na/Ca exchange except Na^+/Na^+ which was found to be electroneutral. iii) $\text{Ca}^{2+}/\text{Ca}^{2+}$ exchange is voltage sensitive even in the absence of external monovalent cations (Li^+ substituted for TRIS or NMG), iv) The affinity of the exchanger towards Na^+ is voltage-insensitive in the range -40 to +20 mV. Our results show that: a) the asymmetric characteristics of the Na/Ca exchange are not the consequence of the asymmetric ionic environment normally prevailing in a living cell but an intrinsic property of the exchanger. b) The fact that $\text{Ca}^{2+}/\text{Ca}^{2+}$ exchange is still voltage-sensitive in the complete absence of external and internal monovalent cations is against the proposition that the voltage sensitivity of the $\text{Ca}^{2+}/\text{Ca}^{2+}$ is induced by the binding of an extra charge on the carrier (external monovalent cation site). (CONICIT, SI-1934, NIH-IR0IHL39243 and TWAS RG No.83-VEN 3).

W-AM-F2 EVIDENCE FOR OCCLUSION OF ANIONS AND CATIONS ON THE Na,K,Cl-COTRANSPORT SYSTEM ISOLATED FROM SHARK RECTAL GLAND. Bliss Forbush III and Mark Haas, with the technical assistance of John T. Barberia and Grace Jones, Mt. Desert Is. Biol. Lab., Salsbury Cove ME, 04672; and Depts. of Physiology and Pathology, Yale University School of Medicine, New Haven, CT 06510.

We have examined the characteristics of binding of [^3H]benzmetanide to membranes isolated from dogfish shark rectal gland. Membranes were prepared as the washed 48000g pellet after homogenization of the gland in 0.25M sucrose/0.25 mM imidazole/35 mM Na/30 mM K/4 mM Cl/20 mM SO_4 /10 mM ATP, and protease inhibitors (stored at -70°C). [^3H]benzmetanide binding (typically ~ 25 pmol/mg protein) is determined by Millipore filtration after incubation of 20 μl samples containing 2-4 mg/ml membrane protein in 10 mM imidazole, 0.02-2 μM [^3H]benzmetanide, and various ions. With 60 mM Na/60 mM K/30 mM Cl/30 mM gluconate/30 mM SO_4 the rate of association of [^3H]benzmetanide is 0.16 $\text{min}^{-1}\mu\text{M}^{-1}$ at 20 °C and the rate of dissociation upon dilution in the same medium is 0.028 min^{-1} ; K_d is ~ 0.175 μM . As previously reported Na, K and Cl are each required for maximal binding, and Cl inhibits at high concentrations. We report that Li can substitute for Na; Cs, NH_4 , or Rb can substitute for K, and (in decreasing order of effectiveness at 50 mM) SCN, Cl, AsO_4 , acetate, F, NO_3 , gluconate, PO_4 , SO_4 , Br, I, and ClO_4 interact at anion sites. NO_3 , AsO_4 , F, PO_4 , SO_4 , acetate, and gluconate appear to interact weakly if at all with the inhibitory anion site. In examining the dissociation of [^3H]benzmetanide from the cotransporter we found that the rate depends to some extent upon ions present in the dissociation medium, but that it depends strongly upon the ions that were present when [^3H]benzmetanide was bound. Thus for instance when Li, acetate, AsO_4 , Rb, NH_4 , or Cs were substituted for their congeners during binding, the rate constant of dissociation (into Na/K/Cl) was 0.012, 0.013, 0.019, 0.020, 0.047, and 0.100 min^{-1} respectively, compared to 0.027 min^{-1} in the control sample. Since the various ions are "remembered" by the transporter, we propose that these ions remain bound at their sites even after the ions are removed from the medium. These results constitute strong evidence that ions are occluded within a transport "pocket" on the Na,K,Cl-cotransport system. (Supported by a Lucille P. Markey fellowship, NIH AM17433, and AHA CT-201-889).

W-AM-F3 STIMULATION OF THE Na,K,Cl-COTRANSPORTER IN THE INTACT SHARK RECTAL GLAND. Bliss Forbush III and Mark Haas, with the technical assistance of Daniel Russett and John T. Barberia, Mt. Desert Is. Biol. Lab., Salsbury Cove ME, 04672; and Depts. of Physiology and Pathology, Yale University School of Medicine, New Haven, CT 06510.

The rectal gland of the dogfish shark is under strong hormonal control: salt secretion increases 10-20 fold above basal levels upon stimulation with vasoactive intestinal peptide (VIP) or various other agents. Previous reports have emphasized the importance of regulation of a Cl channel in the apical membrane of the epithelial cell (Greger et al. *Pflugers Arch.* 402: 376, 1984). In this study we examined [^3H]benzmetanide binding to membranes in the intact gland, in the hopes that binding would reflect availability of active transporter as it does in the avian red cell (Haas and Forbush, *JBC* 261: 8434, 1986). We perfused isolated rectal glands with bicarbonate buffered shark Ringers solution with or without 0.1 mg/l VIP at 18.4°C for 30 min to establish a basal or stimulated rate of salt secretion. Perfusion was continued for an additional 25 min during which 1.0 μM [^3H]benzmetanide (0.1 Ci/mmol) was included in the solution; in most glands secretion was inhibited 60-80% by [^3H]benzmetanide by the end of this period. The gland was homogenized in 5 volumes of 250 mM sucrose/15 mM Na/30 mM K/4 mM Cl/20 mM SO_4 /1 μM unlabeled benzmetanide (and phosphatase and protease inhibitors) at 0°C. Samples of the homogenate were diluted and filtered to determine [^3H]benzmetanide bound to the membranes. We found 11 ± 4 pmol of [^3H]benzmetanide bound per mg total protein in the basal condition (n=5), and 104 ± 9 pmol/mg in the stimulated state (n=5). The evidence that binding is to the Na,K,Cl-cotransport system and is not non-specific binding or uptake into vesicular compartments is: a) non-specific binding would not be strongly regulated, b) binding is not appreciably decreased on hypotonic treatment or freeze-thaw of the membranes, c) dissociation of [^3H]benzmetanide from the membranes has rate constants of 0.02 min^{-1} at 20°C and ~0.003 min^{-1} at 0°C, essentially the same as determined for the Na,K,Cl-cotransport system in other experiments. Our measurements of binding and inhibition of Cl transport give a turnover number of $80 \pm 7 \text{ s}^{-1}$ for the stimulated shark Na,K,Cl-cotransporter at 18.4 °C. These results demonstrate that regulation of the Na,K,Cl-cotransporter is in part responsible for regulation of salt and water secretion by the shark rectal gland. (Supported by a Lucille P. Markey fellowship, NIH AM17433, and AHA CT-201-889).

W-AM-F4 EFFECTS OF LIGANDS ON FLUORESCENCE ENERGY TRANSFER BETWEEN 5-IODOACETAMIDOFLORESCEIN (IAF) AND TRINITROPHENYL-ATP (TNP-ATP) IN (Na,K)-ATPase. P.A. George Fortes and Richard Aguilar, Department of Biology, University of California San Diego, La Jolla, CA 92093-0116.

We have studied the effects of ligands that change the conformation of (Na,K)-ATPase on resonance energy transfer between two probes: TNP-ATP, which binds to the ATP site of the enzyme, and IAF, which reacts with *cys*₄₅₂ without impairing enzyme turnover. We compared the dissociation constant (K_D) for TNP-ATP binding and the efficiency of IAF \rightarrow TNP-ATP energy transfer at saturating TNP-ATP with: 1) No ligands or the presence of NaCl (E_1 form); 2) KCl (20 - 100 mM) to give the K-occluded form, $E_2(K)$; 3) ouabain + Mg + P_i to give the high affinity cardiac glycoside complex (E_2P -ouabain). Although K_D for TNP-ATP (30 nM in the E_1 form) increased 70 - 100-fold in the $E_2(K)$ form and \sim 300-fold in the E_2P -ouabain form, the energy transfer efficiency changed less than 4% under all conditions. The calculated distance between IAF and TNP-ATP was about 24 Å, when the data were corrected for the fraction of functional enzyme in the preparations. This distance changed less than 2 Å in the different conformations. These results indicate either that *cys*₄₅₂ and the ATP site do not move significantly or they move together during the conformational changes that translocate or occlude ions. (Supported by NIH grant RR-08135.)

W-AM-F5 HYPERPOLARIZATION AND EXTERNAL Na REDUCE THE FORWARD RATE OF Na TRANSLLOCATION BY THE Na/K PUMP. R. F. Rakowski, David C. Gadsby and Paul De Weer. Marine Biological Laboratory, Woods Hole, MA 02543.

The influence of hyperpolarization and external Na on the stoichiometry of the Na/K pump was studied in voltage-clamped, internally dialyzed squid giant axons by simultaneously measuring the changes in Na efflux ($\Delta\Phi_{Na}$) and holding current (ΔI) produced by dihydrodigitoxigenin (H_2DTG). As expected for a 3Na/2K pump, the H_2DTG -sensitive $F\Delta\Phi_{Na}/\Delta I$ ratio (F is Faraday's number) was not significantly different ($P > 0.01$) from 3.0 either in Na-free seawater at 0 mV (2.86 ± 0.09 , SEM, $N=8$) or -60 to -90 mV (3.05 ± 0.13 , $N=6$) or in 390 mM-Na seawater at 0 mV (2.72 ± 0.09 , $N=7$) or -60 mV (2.91 ± 0.21 , $N=4$). H_2DTG -induced $\Delta\Phi_{Na}$ and ΔI declined in parallel on hyperpolarization, slightly in Na-free seawater ($13 \pm 5\%$ and $14 \pm 6\%$, respectively over ~ 70 mV) but more steeply in high-Na seawater ($34 \pm 5\%$ and $39 \pm 8\%$ over 60 mV). The results demonstrate that under our conditions of near saturating $[ATP]$, $[K]_o$, and $[Na]_i$ in both Na-free and 390 mM-Na seawater, the Na/K pump transport stoichiometry is 3Na/2K and is independent of membrane potential or of $[Na]_o$. Since net current and unidirectional flux are tightly coupled under these experimental conditions, the decreases in pump rate produced by hyperpolarization or by raising external $[Na]$ must reflect effects on the forward rate of Na translocation rather than on reverse translocation. Supported by NIH grants NS 22979 (RFR), NS 11223 (PDW), HL 36783 and the Irma T. Hirsch Trust (DCG).

W-AM-F6 PROPERTIES OF THE Na/K PUMP IN CHICK CARDIAC MYOCYTES. Stimers, J.R., Shigeto, N. and Lieberman, M. Division of Physiology, Dept. Cell Biology, Duke Univ. Medical Center, Durham NC.

Spontaneously beating aggregates (80-100 μm diameter) of cultured embryonic chick cardiac myocytes were perfused with a modified Hanks' solution and voltage clamped at -70 mV with a single micro-electrode, switching clamp (Dagan model 8100) to measure the Na/K pump current (I_p). Removal of K_o or addition of 1 mM ouabain to the perfusion solution resulted in a rapid (5-10 s) inward shift of the holding current (I_h). In resting steady state preparations the outward ouabain sensitive current was $0.34 \pm 0.05 \mu A/cm^2$ ($n=8$). This value of I_p corresponds to a turnover rate of $23 s^{-1}$ and a Na influx of $11.5 pmol/cm^2 \cdot s$. When K-free solution was used to block I_p , subsequent addition of K_o to activate the Na/K pump generated an outward reactivation current (I_{p-r}), which was ouabain, K_o and Na_i sensitive. By maintaining a preparation in K-free solution with brief (30-60 s) additions of K_o between 0.34 and 10.8 mM, I_{p-r} magnitude was found to be a saturating function of K_o with a Hill coefficient of 2.3 and $K_{0.5}$ of 2.2 mM. I_{p-r} was increased in magnitude when Na_i was increased by increasing the time of exposure to K-free solution prior to reactivation. Steady state I_p was increased more than 3-fold above the resting value to $1.34 \pm 0.23 \mu A/cm^2$ ($n=11$) when Na_i was raised by 3 μM monensin (Na/H ionophore). These results are consistent with I_{p-r} being due to Na/K pump activity. Using these and other published data we calculate that in a resting myocyte I_p should contribute -5.3 mV to the membrane potential and the Na:K coupling ratio is about 1.67:1. We conclude that in cultured embryonic chick cardiac myocytes, the Na/K pump generates a measurable current which, under certain conditions, can be isolated from other membrane currents and has properties similar to those reported for adult cardiac cells. [Supported by NIH grants HL27105, HL17670, HL07063 and HL07101.]

W-AM-F7 N-(2-NITRO-4-ISOTHIOCYANOPHENYL)-IMIDAZOLE INACTIVATION OF THE Na,K-ATPase IN THE Na.E₁ FORM. **Graham C.R. Ellis-Davies** and **Jack H. Kaplan**. Department of Physiology, The University of Pennsylvania, Philadelphia, PA 19104-6085.

Treatment of partially purified Na,K-ATPase from canine renal medulla with a newly synthesized reagent N-(2-nitro-4-isothiocyanophenyl)-imidazole (NIPI) results in inactivation of Na,K-ATPase. The presence in the incubation medium of either Na⁺ or Mg²⁺ potentiates the rate of inactivation by about 10-fold. The inhibition both in the presence and absence of these ligands can be fully protected by ATP or ADP. AMP, K⁺ and 4,4'-dinitro-2,2'-stilbenedisulphonic acid (DNDS) have little effect on the inhibition. At increasing pH NIPI inhibits the enzyme more rapidly. At pH 8.5, 37°C, 5 mM Na⁺, 10 μM NIPI produces 80% inhibition after ca. 10 min. The striking Na⁺ potentiation of inhibition suggests that NIPI is reacting with an amino acid residue (probably a lysine) which is more exposed in the Na.E₁ form than the K.E₂ form of the enzyme. Supported by NIH GM 39500

W-AM-F8 N-ACETYL IMIDAZOLE INACTIVATION OF THE Na,K-ATPASE. **Jose M. Arguello**, and **Jack H. Kaplan**. Department of Physiology, University of Pennsylvania 19104-6085.

Treatment of dog kidney Na,K-ATPase with N-acetyl-imidazole (NAI) produces irreversible inhibition of the Na,K-ATPase and the p-NPPase activities. The I₅₀ for ATPase and p-NPPase activities, at 0° C, 1 hr, are 4.5 mM and 26 mM respectively. ATPase inhibition is only slightly affected by the presence of Na⁺, K⁺, Mg²⁺ or P_i but greatly reduced by ATP (I₅₀ ≈ 8 μM). On the other hand, ATP only slightly protects the inhibition of the p-NPPase activity. The high affinity ADP binding to the enzyme is inhibited to the same extent as the ATPase activity (70%) while phosphorylation by P_i is not altered. Hydroxylamine, a deacetylating reagent for o-acetyl tyrosine but not for n-acetyl lysine, produces incomplete recovery of the enzymatic activity. In spite of the inhibition of high affinity nucleotide binding in NAI treated enzyme, ATP inhibits the p-NPPase activity of both control and modified enzyme with low affinity. This suggests the presence of a low affinity ATP site in the NAI-treated enzyme. Supported by NIH GM39500.

W-AM-F9 RADIATION INACTIVATION ANALYSIS OF OLIGOMERIC STRUCTURE OF THE H,K-ATPASE

Edd C. Rabon¹, Robert D. Gunther¹, Sara Bassilian¹ and Ellis S. Kempner² ¹CURE, VA Center, Wadsworth Division, L A, CA 90073 and The Department of Medicine, UCLA, LA, CA 90024 ²Laboratory of Physical Biology, National Institute of Arthritis and Musculoskeletal and Skin Diseases, National Institutes of Health, Bethesda Maryland, 20892

Target sizes of several functions of the gastric H,K-ATPase were determined in frozen microsomal vesicles irradiated with high energy electrons. For each parameter, the combined data points of three experiments, was fitted by an exponential function of radiation dose to less than 10% of the initial value. Target sizes fell into three groups. The lowest group of target sizes described peptide destruction (determined by loss of Coomassie blue staining of the monomer region of SDS PAGE) with a size range of 92-145 k daltons and the loss of the MgATP-dependent phosphoenzyme with a size range of 133-146 k daltons. A larger group of target sizes described the loss of catalytic activities including the K⁺ phosphatase and the K⁺-stimulated ATPase. These catalytic functions exhibited target sizes of 200±13 k daltons and 232±23 k daltons, respectively. Passive Rb⁺ exchange and active H⁺ transport in reconstituted proteoliposomes exhibited target sizes of 233_{n=2} and 388±48 kDa, respectively. The lower target size group represents the first evidence that partial enzyme function resides in the monomer of the H,K-ATPase. The intermediate group of target sizes suggests that subunit interactions do contribute to full cycle catalytic activity. Subunit interactions appear necessary for all ion transport activities.

W-AM-F10 Tl-201 UPTAKE MONITORS MEMBRANE POTENTIAL IN HUMAN GLIOMA CELLS. T. Brismar¹, V.P. Collins² and M. Kesselberg³. ¹Dept of Clin Neurophysiol., ²Ludwig Institute for Cancer Research, Karolinska Hospital, Stockholm and ³Dept of Physics, Univ. of Stockholm, Sweden.

The mechanism for the cellular uptake of thallium-201 was studied in vitro on human glioma cells. This was of interest since Tl-201 uptake (in vivo) is used in clinical medicine for the diagnosis of brain tumors (and myocardial function). The results indicated that Tl-201 may become a useful probe for membrane potential measurements.

The external concentration of K⁺, Tl⁺ and Rb⁺ affected the uptake of Tl-201. Between 3 and 50 mM-K⁺ the Tl-201 uptake (after 60 min incubation) was inversely proportional to external [K⁺] as predicted by the Nernst equation when the cells have a high K-selectivity in the membrane. Using uptake in isotonic KCl as reference (0 mV), the calculated membrane potential was -75 mV in a medium with 3 mM-K⁺. Addition of non-radioactive Tl⁺ decreased the uptake of Tl-201 in a similar fashion as K⁺, but its effectiveness was about 7 x higher, indicating a similar ratio between the ion permeabilities (P). Changes in external [Rb⁺] suggested that P_{Tl}:P_{Rb} was 4-5, and a similar ratio was calculated from comparison of the time course for Rb-86 uptake with Tl-201 uptake. Ouabain (1 mM) decreased the uptake to 60 % at steady state. The time course for the uptake was faster in the presence of ouabain (half time 7-8 min) than in standard medium (10-15 min). This effect was explained by the depolarisation caused by ouabain.

It was concluded that Tl-201 is not transported into these cells by a Na/K(Tl) ATPase dependent pump, but its distribution depends on the membrane potential gradient in a K (Tl) permeable membrane. Since all studied cells have P_{Tl} > P_{Rb}, Tl-201 may become a more useful probe than Rb-86 for membrane potential measurements in cell populations.

W-AM-F11 IDENTIFICATION OF THREE DISULFIDE BONDS AND ONE FREE SULFHYDRYL IN THE β SUBUNIT OF (Na,K)-ATPase. T.L. Kirley, Department of Pharmacology and Cell Biophysics, Univ. of Cincinnati, Cincinnati, Ohio 45267-0575.

The physiological role of the β subunit in (Na,K)-ATPase has yet to be established. However, disulfide bond(s) in the β subunit have been suggested to be essential for enzymatic activity (Kawamura and Nagano, BBA 774, 188-192 (1984)). In order to determine the oxidation state of the seven cys residues present in the beta subunit of lamb kidney (Na,K)-ATPase, a reactive sulhydryl group directed reagent, 4-(aminosulfonyl)-7-fluoro-2,1,3-benzoxadiazole (ABD-F), was used to label the cysteine residues, both before and after reduction of disulfide bonds. The results indicated that only one cysteine residue exists in the β subunit, ⁴⁴cys, which is located in the single transmembrane domain predicted to exist in the β subunit. The other 6 cys residues are involved in 3 disulfide bonds as proven by sequence analysis of tryptic peptides. Thus, ¹²⁵cys is disulfide linked to ¹⁴⁸cys, ¹⁵⁸cys to ¹⁷⁴cys, and ²¹²cys to ²⁷⁵cys. This is in sharp contrast to the α subunit, where apparently all 23 cys residues exist as free sulfhydryls. The single free sulfhydryl in β (⁴⁴cys) is fairly unreactive, presumably due to its location deep within the membrane, explaining the total lack of labelling of the β subunit by sulfhydryl directed chemical modification reagents in the absence of denaturing conditions. Previously, in dog kidney (Na,K)-ATPase, Ohta et al (FEBS Lett 204, 297-301 (1986)) had identified a single disulfide bond present in β corresponding to ¹⁵⁸cys to ¹⁷⁴cys in lamb kidney (Na,K)-ATPase. Which, if any, of the 3 disulfides in β is "essential" for (Na,K)-ATPase activity is not clear at this time. Supported by grant #SW-88-24 from the Ohio Affiliate of the AHA and NIH P01 HL22619.

W-AM-F12 FLUORESCENCE ENERGY TRANSFER STUDIES ON ERYTHROCYTE Ca²⁺-ATPase.

D. Kosk-Kosicka, T. Bzdega, and A. Wawrzynow. University of Maryland, School of Medicine, Department of Biochemistry, 660 W. Redwood, Baltimore.

The studies were performed on Ca²⁺-ATPase purified from erythrocyte ghost membranes, after labeling with one of three fluorescent probes: fluorescein-5'-isothiocyanate (FITC), tetramethylrhodamine-5-isothiocyanate (TRITC) or eosin-5-maleimide. All three probes revealed binding stoichiometry close to 1:1. Fluorescence energy transfer was measured between the modified enzyme molecules from FITC to TRITC, and from FITC to eosin-5-maleimide. The highest efficiency of the energy transfer was 12% and 10%, respectively. The dependence of the amount of energy transfer on enzyme concentration, half-maximal at 15-20 nM enzyme, showed considerable resemblance to the previously reported dependence of Ca²⁺-ATPase activity and fluorescence polarization of the FITC-modified enzyme. Thus both energy transfer and polarization measurements are reporting the same phenomenon: enzyme self-association that causes full activation of the Ca²⁺-ATPase activity and is independent of calmodulin. Taking into account the Forster critical distance the values calculated from maximal energy transfer suggest that the enzyme monomers self-associate in such a way that the apparent distance between lysines 601 on two enzyme molecules is around 65 Å, whereas the apparent distance between the lysine on one and a maleimide-reactive cysteine on another molecule is around 77 Å. Supported by NIH GM37143.

W-AM-G1 A VOLTAGE-DEPENDENT CHLORIDE CHANNEL IN THE PHOTOSYNTHETIC MEMBRANE OF A HIGHER PLANT. R. Hedrich⁺, G. Schönknecht^{*}, W. Junge^{*} and K. Raschke⁺.
⁺Pflanzenphysiologisches Institut der Universität Göttingen, 3400 Göttingen, West Germany, and
^{*}Biophysik, FB Biologie/Chemie, Universität Osnabrück, 4500 Osnabrück, West Germany.

Photophosphorylation in photosynthetic membranes of plants (thylakoid membranes) is driven by an electrochemical potential difference of the proton. The light driven net uptake of protons into the thylakoid lumen is electrically balanced by the motion of other ions. Whether Mg⁺⁺ or Cl⁻ are involved, or both, is under debate. We used patch-clamp techniques to study the molecular mechanism of ion transport in thylakoids. In isolated membrane patches from osmotically inflated thylakoids of *Peperomia metallica* a voltage-dependent, anion-selective, channel was discovered. At 30 mM Cl⁻ the single-channel conductance was 65 pS, showing ohmic behaviour between -80 and +80 mV. The opening probability was maximal at about +40 mV (inside the thylakoid). Application of voltage steps caused additional superimposed transient channel openings. This chloride channel could provide a mechanism involved in charge-balancing during light-driven proton uptake by thylakoids.

W-AM-G2 ELECTRON SPIN-LATTICE RELAXATION OF THE STABLE TYROSINE RADICAL IN PHOTOSYSTEM II. Warren E. Beck and Gary W. Brudvig, Department of Chemistry, Yale University, New Haven, Connecticut 06511.

The electron spin-lattice relaxation of the stable tyrosine radical D⁺, located at Tyr-160 in the D2 polypeptide of photosystem II, has been studied through pulsed saturation-recovery experiments over the 3.8-120 K range. Compared to the spin-lattice relaxation of a model tyrosine radical generated in a glass by UV irradiation, the relaxation of D⁺ is two orders of magnitude more rapid at the lowest temperatures. Removal of functional Mn ions from the O₂-evolving center does not cause a significant decrease in the relaxation rate compared to that observed in the S₁ state with the Mn complex intact. In addition, oxidation of the O₂-evolving center to the S₂ state causes only a modest enhancement in the relaxation rate of D⁺, indicating that only a weak magnetic interaction with the Mn complex is present. At temperatures below 50 K, the spin-lattice relaxation of D⁺ occurs with complex, non-exponential kinetics; however, a transition to exponential relaxation kinetics is observed as the temperature is raised above 50-60 K. The transition to single-exponential relaxation kinetics does not occur with a significant change in the EPR line shape of D⁺, as judged from continuous-wave spectra and from time-resolved spectra obtained by gated detection of saturation-recovery transients, ruling out the possibility that motional averaging of two or more conformations could account for the temperature-dependent relaxation behavior. We suggest that the relaxation kinetics of D⁺ are instead dominated at low temperatures by a dipolar interaction with a paramagnetic site other than the Mn complex, resulting in a deviation from single-exponential relaxation kinetics, while at higher temperatures the intrinsic spin-lattice relaxation process is dominant, resulting in single-exponential relaxation kinetics. [Work supported by NIH grant GM36442.]

W-AM-G3 EPR SPECTRA OF SELECTIVELY DEUTERATED TYROSINE RADICALS. Mohamed K. El-Deeb,¹ Bridgette A. Barry² and G.T. Babcock.¹

¹Department of Chemistry, Michigan State University, E. Lansing, MI 48824 and ²Department of Biochemistry, University of Minnesota, St. Paul, Minnesota, 55108. (Introduced by Charles F. Yocum.)

Since it became evident that tyrosine radicals are involved in the photosynthetic process, and that a tyrosine radical is what gives rise to the EPR signal II (Barry and Babcock (1987), PNAS 84, 7099), it has been our interest to investigate, in more detail, the nature of those radicals in their protein environment. By *in vivo* selective deuteration, it has been shown that the EPR spectrum of D⁺ in cyanobacteria is dramatically changed by deuteration at the methylene position and at the 3,5 positions of the aromatic ring, whereas no significant change in the spectrum was observed upon deuteration at the 2,6 positions (Barry *et al* (1988), Biophys. J. 53 (2), pt. 2, 616a). For comparison, we have generated tyrosine radicals by UV photolysis of frozen selectively deuterated samples. Our results indicate that the major spin density is at carbons 1,3,5 of the aromatic ring, in agreement with the data from D⁺ and single crystal studies. However, different methylene proton couplings were observed in tyrosine model compounds, D⁺, and tyrosine in ribonucleotidediphosphate reductase (RDPR), which we attribute to different conformations of the methylene protons. This work was supported by NIH (GM 37300) and the USDA photosynthesis program.

W-AM-G4 THE CATALYTIC ROLE OF THE MR=17 KD PROTEIN IN CHLOROPLAST CYTOCHROME b_6-f COMPLEX. Li, L.-B., Yu, L., and Yu, C. A., Department of Biochemistry, OAES, Oklahoma State University, Stillwater, OK 74078

Purified spinach chloroplast cytochrome b_6-f complex contains four polypeptides with molecular weights of 33, 23.5, 20, and 17 Kd. The first three polypeptides are identified as cytochrome f , cytochrome b_6 , and Rieske's iron sulfur protein. The 17 Kd protein has recently been identified as plastoquinone binding protein through the photoaffinity labeling study using an azido-quinone derivative. The purified complex catalyzes the electron transfer from plastoquinol to cytochrome c at the rate of 35 μ moles cytochrome c reduced per nmol cytochrome f per hour, at room temperature. The activity is sensitive to treatment with trypsin. When the purified cytochrome b_6-f complex, 1 mg/ml, in 50 mM Tris-Succinate buffer, pH 7.0, containing 0.1% sodium cholate, was incubated with trypsin (80 μ g/mg protein) at room temperature for different lengths of time, the enzymatic activity decreased as the incubation time increased. The maximal inactivation of 75% was reached at 8 min. No change in absorption spectral properties was observed when the digested complex was compared with the intact complex; however, when the trypsin-treated samples were analyzed by SDS-PAGE, the 17 Kd protein disappeared, but the other proteins were relatively intact, suggesting that the inactivation by trypsin is due to the digestion of the 17 Kd protein of the cytochrome b_6-f complex and not to the other redox components. Since the 17 Kd protein is identified as the plastoquinone binding site, destruction of this protein would certainly interfere with plastoquinone binding and thus cause the inactivation. The effect of the trypsin treatment on EPR characteristics of cytochrome b_6 , cytochrome f , iron sulfur center, and plastosemiquinone radical will be reported. (Supported in part by grant from USDA).

W-AM-G5 MUTATIONS AT THE Q_A BINDING SITE IN *Rhodobacter capsulatus* REACTION CENTERS AFFECT QUINONE BINDING AND ELECTRON TRANSFER. William J. Coleman, Edward J. Bylina and Douglas C. Youvan, Department of Chemistry, Massachusetts Institute of Technology, Cambridge, MA 02139 U.S.A.

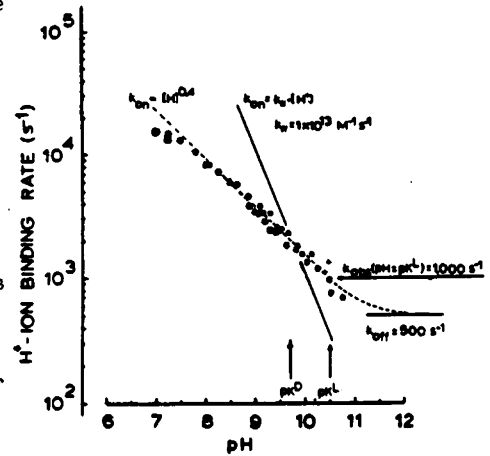
Directed mutations were introduced at histidine 217 (H217) and tryptophan 250 (W250) in the M subunit of the *Rhodobacter capsulatus* photosynthetic reaction center complex in order to examine the role of these residues in electron transfer at the primary quinone (Q_A). RCs isolated from several of the mutants (H \rightarrow C,D,E,Q,A,L or M) and (W \rightarrow E,R,T,V,L or M) were lacking a substantial fraction of Q_A , as indicated by the extent of bleaching of the long-wavelength absorption band of the special pair under continuous actinic illumination. Although adding exogenous quinone (such as 2-Methyl-1,4-naphthoquinone) restored complete bleaching during continuous illumination, in general these mutants differ significantly from wild-type, in that: 1) the apparent RC affinity for quinone is greatly reduced; 2) the flash-induced yield of $P^+Q_A^-$ is reduced; and 3) the recovery of P after bleaching by a single flash is much slower.

W-AM-G6 ROLE OF BICARBONATE IN PHOTOSYNTHETIC SYSTEMS. Govindjee, Departments of Physiology and Biophysics and Plant Biology, University of Illinois, Urbana, IL.61801

Bicarbonate has been shown to be required for electron flow in thylakoids from plants (Blubaugh and Govindjee, *Biochim. Biophys. Acta*, 848, 147-151, 1986; 1988, in press), and from cyanobacteria (J. Cao and Govindjee, *Photosynthesis Research*, 1988, in press). However, photosynthetic bacteria do not show any effect of bicarbonate-depletion on any of their electron transfer reactions (R.J. Shopes, D.J. Blubaugh, C.A. Wraight and Govindjee, *Biochim. Biophys. Acta*, 1988 submitted). The bicarbonate effect in plants is located on the electron acceptor complex Q_A-Fe-Q_B , the "two electron gate," of photosystem II, and is pH dependent (J. Eaton-Rye and Govindjee, *Biochim. Biophys. Acta*, 1988, in press). It is suggested that there are two binding sites of HCO_3^- : one on Fe, and the other on an arginine near Q_B ; they function to stabilize the reaction center complex and to provide protons to Q_B^- (Blubaugh and Govindjee, *Photosynthesis Research* 19, 85-128, 1988). Photosynthetic bacteria, however, substitute a glutamic acid for bicarbonate in their binding to Fe (H. Michel and J. Deisenhofer, *Biochemistry* 27, 1-7, 1988). Perhaps, the binding site on Fe is also responsible for a site of HCO_3^- between the electron donor "Z" and " Q_A " recently observed in leaf discs from spinach (F. El-Shintinawy and Govindjee, paper in preparation). I thank D. Blubaugh, J. Cao, R.J. Shopes, J. Eaton-Rye and F. El-Shintinawy for their collaboration in this research.

W-AM-G7 ANOMALOUS KINETICS OF FLASH-INDUCED H⁺-ION BINDING IN REACTION CENTERS FROM RB. SPHAEROIDES. Peter Maroti and Colin A. Wraight, Department of Plant Biology, University of Illinois, Urbana, IL 61801 (Introduced by W. J. Williams).

Electron transfer events, especially the reduction of the quinone acceptor complex in the reaction center (RC) of photosynthetic bacteria, are associated with H⁺-ion binding. The kinetics of proton binding by RC after flash excitation were measured with two completely independent methods: spectroscopically with wide range of pH indicator dyes and electrically with conductance changes. Several remarkable kinetic features were revealed: the rate was (1) extremely fast, (2) deviated from linearity with respect to the external (bulk) proton concentration (see figure for terbutryn-blocked RC) and (3) was affected largely by ionic screening and (4) by deuterium exchange and (5) the kinetics were complex in Q_B-active RC. These experimental evidences demonstrate the significance of the electrostatic profile (electrostatic focusing of the protons to the amino acid residues) and of the conformational fluctuations (degrees of accessibility of partially buried protonatable groups) of the protein.



This work has been supported by NSF grant DMB 86-17144.

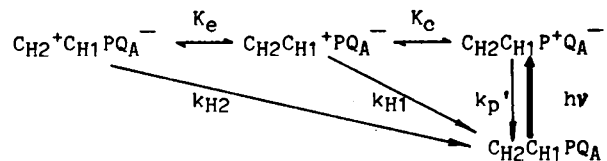
W-AM-G8 DELETION MUTATION OF THE PHOTOSYNTHETIC REACTION CENTER OF RHODOBACTER SPHAEROIDES AND COMPLEMENTATION WITH MODIFIED REACTION CENTER GENES. Eiji Takahashi¹ and Colin A. Wraight^{1,2} Department of Plant Biology¹ and Department of Physiology and Biophysics², University of Illinois, Urbana, Illinois, 61801. (Introduced by John Whitmarsh)

The photosynthetic reaction center is a protein-pigment complex where the primary photochemical electron transfer occurs. We are currently probing the relationship between molecular organization and biophysical activity of the reaction center from *Rhodobacter sphaeroides* using the techniques of site-directed mutagenesis, accompanied by spectroscopic and kinetic characterization of the altered complexes. Chromosomal deletion mutants of the reaction center (RC-) were created in the wild-type *Rb. sphaeroides* (2.4.1.), as well as in the Ga and R26 strains. The deletion eliminates most of the coding regions of the L and M subunits of the reaction center. The resulting deletion mutants are photosynthetically incompetent and cannot grow in the light, but can grow heterotrophically in the dark. When the wild-type reaction center genes are introduced into the RC- mutants, *in trans*, on a stable plasmid, photosynthetic growth is restored. In addition, when reaction center genes isolated from herbicide resistant strains of *Rb. sphaeroides* were introduced into the RC- mutants, they acquired herbicide resistance. We have also successfully complemented the RC- mutants with genes containing site-directed mutations of amino acid residues in the Q_B-binding region of the L subunit. The electron transfer properties of the isolated mutant reaction centers will also be presented. This work was supported by grants from the McKnight Foundation and NSF DMB 86-17144.

W-AM-G9 THE CHARGE RECOMBINATION PATHWAYS OF C_{H2}⁺PQ_A⁻ AND THEIR FREE ENERGY AND KINETIC RELATIONS IN RCs FROM *Rp. VIRIDIS*. Jiliang Gao, Robert J. Shopes and Colin A. Wraight, University of Illinois, Urbana, IL 61801. (Introduced by Rajni Govindjee)

The electron transfer reactions and thermodynamic equilibrium involving the high potential cytochromes c (C_{H1} and C_{H2}) and primary quinone acceptor Q_A in reaction centers from *Rhodospseudomonas viridis* were investigated. A scheme of the reactions is suggested as shown. After a flash, the charge recombination rate of the state, C_{H2}⁺C_{H1}PQ_A⁻, was calculated by

$k_{H2}^{app} = [k_p' + K_c(k_{H1} + K_e k_{H2})] / [1 + K_c(1 + K_e)]$. If, however, C_{H2} was oxidized before the flash the decay rate of the state, C_{H2}⁺C_{H1}PQ_A⁻, was derived as $k_{H1}^{app} = (k_p' + K_c k_{H1}) / (1 + K_c)$. The equilibrium constants, K_c and K_e, were taken from the difference in the corresponding measured equilibrium midpoint potentials, the rate of P⁺Q_A⁻ decay, k_p', the rate when the high potential cytochromes c were reduced, and k_{H2} and k_{H1} were taken from the measured rates at low temperature where the rates were constant. All three variable parameters were measured over a range of pH and temperature. We got good agreement between theory and experiment, which indicated that there were no significant electrostatic interactions between the relevant redox centers in isolated RCs, i.e., the effective dielectric constants were high. This work was supported by the NSF (DMB 86-17144).



W-AM-H1 ENERGY ANALYSIS AND HYDROPHOBICITY OF SICKLE HEMOGLOBIN PARACRYSTALS

Stanley J. Watowich and Robert Josephs

Department of Molecular Genetics and Cell Biology, University of Chicago, Chicago, Illinois 60637.

Under physiological conditions sickle hemoglobin (HbS) molecules aggregate to form long helical fibers. *In vitro* several well characterized polymorphic intermediates are observed during the transition from fibers to crystals. Electron microscopic and x-ray diffraction studies have shown the common structural motif in the HbS fibers, intermediate polymers and crystals is the Wishner-Love double strand. The double strand is composed of two strands of HbS molecules; molecules in the first strand are related to molecules in the second strand by an approximate noncrystallographic two-fold screw axis. In the HbS fiber and intermediates the double strands are axially shifted and twisted whereas in the crystal the double strands are aligned and linear. Thus the transition from fibers to crystals appears to involve a progressive shifting and unwinding of the Wishner-Love double strands.

To understand the structure of the HbS polymers and the mechanism of double strand rearrangement we have studied the transition from an HbS intermediate, termed a paracrystal, to the HbS crystal. The double strands in paracrystals display crystalline order along the *b*- and *c*-axis and a noncrystalline bimodal distribution of translational displacements along the *a*-axis. The peaks of the distribution are -6Å and 20Å from the crystalline positions. We performed a series of adiabatic energy minimizations and locally constrained molecular dynamics calculations on the HbS crystal, translating the double strands along the *a*-axis to simulate the paracrystal disorder. Local minima in the resulting energy profile reproduced the observed paracrystal displacements. The energy minimum at the -14Å displacement is stabilized by intermolecular electrostatic interactions while the energy minimum at the 20Å displacement appears stabilized by changes in intramolecular interactions. In addition, the hydrophobicity of the solvent accessible surface area of the crystal was calculated during the double strand translations and correlates with the displacements observed in paracrystals. Supported by NIH grants HL0227 (SJW) and HL22654 (RJ).

W-AM-H2 HELICAL STRUCTURE DETERMINATION FROM TILTED HbS FIBER CROSS-SECTIONS.

Michael R. Lewis, Thomas E. Lee, and Robert Josephs, Laboratory for Image Analysis and Electron Microscopy,

Department of Molecular Genetics and Cell Biology, University of Chicago, Chicago IL 60637

Sickle-cell anemia is caused by intracellular formation of deoxyhemoglobin S (HbS) fibers. The structure of HbS fibers has been reconstructed to 32 Ångstroms resolution from electron micrographs of negatively stained particles. Additional information about the fiber structure can be obtained from micrographs of embedded and sectioned fibers which present end-on views of a particle. A micrograph in which the particle axis is slightly tilted contains a partial set of three-dimensional data. By applying appropriate additional constraints (in this case the known electron density of HbS and molecular co-ordinates of the fiber) we can use these data to refine the fiber structure.

Micrographs of fiber cross-sections are exquisitely sensitive to particle orientation. Even a small change (ca. a few degrees) in orientation produces a marked difference in their appearance. This sensitivity makes the recovery of three dimensional information a practical possibility. In this work we show that the complicated superimposition pattern resulting from convolution of the HbS molecule with the projection of a tilted helical lattice is accurately described by a rotation about a center which is uniquely determined only by the axis tilt angle and helix handedness. By applying the constraints mentioned above, we have used this property to determine the handedness of HbS fibers and to determine the tilt angle of cross-sections. The molecular details of the fiber structure can be recovered from micrographs of cross-sections by rotational deconvolution of the pattern about this center. We have characterized the rotational deconvolution algorithm with model studies and we are using it to obtain the partial three-dimensional data from micrographs of HbS fiber cross-sections.

This work has been supported by NIH grant HL22654 (RJ).

W-AM-H3 DETERMINATION OF HbS FIBER ORIENTATION IN CROSS-SECTIONS USING CORRESPONDENCE ANALYSIS

T. E. Lee, M. R. Lewis, and R. Josephs. Laboratory for Electron Microscopy and Image Analysis.

Department of Molecular Genetics and Cell Biology, University of Chicago, Chicago Illinois 60637

Upon deoxygenation sickle hemoglobin (HbS) polymerizes into long helical fibers. Within red cells these fibers align into bundles which distort and rigidify the cell initiating the cascade of pathophysiological events characteristic of sickle cell anemia. Bundle assembly is an example of a class of reactions in which macromolecules associate to form larger, more complex structures. We are making a detailed analysis of fiber packing within HbS bundles using transmission electron microscopy of bundle cross-sections which present end-on views of the individual fibers. Ideally a cross-section is a projection down the fiber axis, but in practice the precise orientations of the particles are unknown because the section rarely lies perfectly flat on the electron microscope grid and the plane of sectioning is generally not exactly normal to the particle axis. However, a structural analysis of fiber packing in a bundle requires a precise knowledge of the fiber orientation. We are using correspondence analysis to determine the fiber orientations in these cross-sections.

Applying correspondence analysis to fiber images within a cross-section segregates the particles into groups having the same appearance. The task is to determine the particle orientations that the groups represent. We accomplish this by applying correspondence analysis to models of fibers representing a series of orientations. Plotting the models within the first few dimensions determined by correspondence analysis provides references for this space. Fiber images of unknown orientation can then be plotted in the same space as the models. By noting the plotting locus of the fibers in relation to the models, the orientation of the fibers can be determined.

This work was supported by NIH grant HL22654(RJ).

W-AM-H4 BIOPHYSICAL CHARACTERIZATION OF THE MICELLAR PROPERTIES OF ALPHA-CRYSTALLIN AGGREGATES. Jane F. Koretz, Center for Biophysics and Dept. of Biology, Rensselaer Polytechnic Inst., Troy, NY, and Robert C. Augusteyn, Dept. of Biochemistry, Univ. of Melbourne, Parkville, Victoria.

Alpha-crystallin, the major protein of the mammalian eye lens, has been suggested to exhibit micellar aggregation properties (Augusteyn and Koretz, 1987, FEBS Lett.) rather than a unique structure or set of structures. Characterization of the alpha-crystallin elution profile from a gel filtration column shows a range of structures across the peak - spheres, gradually lengthening rods, and sheets - consistent with this hypothesis (Augusteyn and Koretz, submitted). To test this hypothesis further, the time-dependent effects of increased hydrostatic pressure on aggregate size, the effect of temperature on reconstituted alpha-crystallin, and the effect of increasing concentration of alpha-crystallin on solvent surface tension were investigated. Upon increased hydrostatic pressure, the turbidity of alpha-crystallin also increases, reaching a plateau at about 8000 psi; upon pressure release, the turbidity very slowly returns to its initial levels. In the reconstitution experiments, increasing temperature was associated with a gradual increase in the number and size of sheetlike aggregates relative to smaller spheroidal structures. Finally, over a concentration range from femtomolar to micromolar, alpha-crystallin had no effect on solvent surface tension, while other control proteins demonstrated the expected effects. All of these observations are inconsistent with the classic condensation-polymerization mechanism by which most aggregating proteins seem to be governed. They ARE consistent, however, with the behavior expected of amphiphiles that aggregate into micelles.

Support in part by NIH grant EY02195 to JFK.

W-AM-H5 THE NATURE OF ELECTROSTATIC REPULSION FORCES IN THE ANOMALOUS TEMPERATURE DEPENDENCY OF SWELLING PRESSURE IN THE MAMMALIAN CORNEAL STROMA. L. Stephen Kwok and Stephen D. Klyce, Lions Eye Research Laboratories, LSU Eye Center, 2020 Gravier St, Suite B, New Orleans LA 70112.

The mammalian corneal stroma exerts an expansive swelling pressure of ~ 60 mmHg (~ 8 kPa) under free-swelling conditions. Results from our laboratory indicate that Donnan swelling theory satisfactorily accounts for substantial excursions in stromal hydration in physiological saline. However, the macroscopic Donnan model predicts a positive temperature dependency of the swelling pressure (SP), at variance with Hara & Maurice (1972). Brenner & Parsegian (1976) attempted to explain the anomalous (negative) temperature dependency of SP by applying the Parsegian & Gingell (1972) model based on Poisson-Boltzmann theory for parallel-plate double layers. They reported that $(d \ln SP/dT) = -1.0 \text{ Pa K}^{-1}$ implied a stromal fixed charge concentration $n_f > 3 \text{ mole e}^-/l$, far in excess of known estimates of 0.05 to 0.06 mole e^-/l for the stoichiometric macroion charge. Even when $(d \ln SP/dT) = 0$, Brenner & Parsegian predicted $n_f = 0.18 \text{ mole e}^-/l$. The neglect of ion-ion correlations and the effect of finite ion size may be a factor. However, we have extended the approach, and report that $n_f = 0.06 \text{ mole e}^-/l$ can account for both negative and positive values of $(d \ln SP/dT)$. We have assumed that surface charge density σ is not constant, but changes with temperature T . For $(d \ln SP/dT)$ in the range $(-1.0 \text{ to } +0.7)$, we predict that $d \ln \sigma/dT < 0$. The mechanism whereby surface charge density would rise with decreased temperature is unknown. We hypothesize that entropic changes occur in the glycosaminoglycans and the distribution of charges, such that local charge density is increased at reduced temperature. (Supported by U.S. PHS grant EY03311 from NEI.)

W-AM-H6 AT WHAT STAGE IN THE POLYMERIZATION OF SUBUNITS INTO ICOSAHEDRAL SHELLS IS THE QUASI-EQUIVALENT BONDING SPECIFIED? Peter Prevelige, Dennis Thomas & Jonathan King. Dept of Biology, MIT, Cambridge, MA. 02139

For spherical viruses composed of identical subunits, the subunits at the fivefold vertices must be packed differently than the subunits which are sixfold coordinated. Thus identical subunits must take up different conformations. How do identical polypeptide chains under identical solvent conditions know which conformation to take?

In the dsDNA phage this process requires the presence of a helper species- the scaffolding protein- which ensures the correct organization of the coat protein into closed shells. We have recently developed conditions under which the reaction proceeds in vitro with high efficiency, and shown that this reaction requires the copolymerization of coat and scaffolding subunits.

One possible pathway for generating different packings would be the formation of pentameric and hexameric oligomers from two slightly different conformation in solution, followed by polymerization of these into shells. Such models assume formation of unstable incorrect structures, and reshuffling to the lowest energy icosahedral structure.

Under assembly conditions we find no evidence for association of either coat subunits or scaffolding subunits into pentameric or hexameric complexes. Since coat and scaffolding interaction is required for polymerization, it is possible that conformation specification occurs in the formation of fivefold and sixfold mixed oligomers. However, we have been unable to detect any oligomeric species. The overall kinetics of the reaction show no evidence of a lag during which intermediates build up. All of the results can be fit by a model in which monomers or dimers add to the growing edge, where all the regulatory interactions occur.

W-AM-H7 COMPOSITION OF SECRETORY GRANULES BY ELECTRON PROBE MICROANALYSIS OF CRYOSECTIONED RAT PANCREATIC ISLETS. Margaret C. Foster, Richard D. Leapman, Min Xu Li, Richard L. Ormberg, Illani Atwater, BEIB, DRS and LCBG, NIDDK, National Institutes of Health, Bethesda, Md. 20892.

Electron probe microanalysis of islets allows variability as well as averages of granule composition to be assessed in both alpha and beta cells *in situ*. Islets were isolated by collagenase digestion from adult rats and incubated for 2 to 3 hours in culture medium at 37° C in the presence of 5.6 mmol/l glucose. Several islets were transferred to a Balzers freeze-fracture "hat" that was adapted with filter paper to absorb excess liquid. Within 20 seconds of transfer, the islets were frozen on the liquid helium-cooled block of a Medvac Cryopress freezing machine. Sections for analysis, 100 nm thick, were taken from within the first 20 μm of the frozen surface. Analyses were obtained from approximately 50 nm diameter regions of the sample. Secretory granules in some cells contain high levels of sulphur and zinc, attributable to insulin-containing granules in beta cells. Secretory granules in other cells contain low levels of sulphur and no detectable zinc, attributable to glucagon-containing granules in alpha cells, which are found in high density at the surface of rat islets. The phosphorus content was high in granules of both alpha and beta cells, consistent with other observations that ATP is concentrated in secretory granules. Preliminary estimates indicate that the zinc content of beta granules is approximately 30 mmol/kg dry weight and the sulphur content approximately 300 mmol/kg dry weight, corresponding to approximately 50 mmol/kg dry weight insulin. No detectable zinc was found in the nucleus or cytoplasm. Calcium in granules from the same cell ranged from 10 to 50 mmol/kg dry weight, and in nuclei was less than 2 mmol/kg dry weight. These data support the hypothesis that zinc and calcium are associated with insulin in granules of beta cells *in situ*.